ELSEVIER

Agricultural and Forest Meteorology 101 (2000) 265–289

AGRICULTURAL AND FOREST METEOROLOGY

www.elsevier.com/locate/agrformet

An analytical model for estimating canopy transpiration and carbon assimilation fluxes based on canopy light-use efficiency

M.C. Anderson [a,*], J.M. Norman [a], T.P. Meyers [b], G.R. Diak [c]

[a] *Department of Soil Science, University of Wisconsin-Madison, 1525 Observatory Drive, Madison, WI 53706, USA*

[b] *NOAA/ATDD, 456 South Illinois Avenue, Oak Ridge, TN 37830, USA*

[c] *Cooperative Institute for Meteorological Satellite Studies, University of Wisconsin-Madison, 1225 West Dayton Street, Madison, WI 53706, USA*

Received 29 March 1999; received in revised form 28 October 1999; accepted 9 December 1999

Abstract

We develop a simple, analytical model for canopy resistance to canopy–atmosphere gas exchange that is well suited for incorporation into regional-scale land-surface parameterizations. This model exploits the conservative nature of canopy light-use efficiency (LUE) in carbon assimilation that is observed within broad categories of plant species. The model paradigm assumes that under standard environmental conditions, a canopy will operate at the field-measured LUE, but will deviate from this standard efficiency as conditions change. Effective LUE estimates generated by the model respond to variations in atmospheric humidity, CO_2 concentration, the composition of solar irradiation (direct versus diffuse beam fractions), and soil moisture content. This modeling approach differs from scaled-leaf parameterizations in that a single estimate of nominal canopy LUE replaces both a detailed mechanistic description of leaf-level photosynthetic processes and the scaling of these processes from the leaf to canopy level. This results in a model that can be evaluated analytically, and is thus computationally efficient and requires few species-specific parameters. Both qualities lend themselves well to regional-and global-scale modeling efforts. For purposes of testing, this canopy resistance submodel has been embedded in the Atmosphere–Land Exchange (ALEX) surface energy balance model. The integrated model generates transpiration and carbon assimilation fluxes that compare well with estimates from iterative mechanistic photosynthetic models, and with flux measurements made in stands of corn, soybean, prairie grasses, desert shrubs, rangeland, and black spruce. Comparisons between modeled and measured evapotranspiration (LE) and carbon assimilation (A_c) fluxes yield mean-absolute-percent-differences of 24% (LE) and 33% (A_c) for hourly daytime fluxes, and 12% (LE) and 18% (A_c) for daily-integrated fluxes. These comparisons demonstrate robustness over a variety of vegetative and climatic regimes, suggesting that this simple analytical model of canopy resistance will be useful in regional-scale flux evaluations.

Keywords: Canopy; Carbon assimilation; Evapotranspiration; Light-use efficiency; ALEX

1. Introduction

Stomata simultaneously regulate both the influx of carbon dioxide and the efflux of water between a leaf and its environment, constantly modifying the resistance to gas exchange in response to changing environmental conditions to maintain plant growth

* Corresponding author. Tel.: +1-608-265-3288; fax: +1-608-265-2595.
E-mail address: anderson@bob.soils.wisc.edu (M.C. Anderson).

0168-1923/00/$ – see front matter
PII: S0168-1923(99)00170-7

while minimizing water loss. On the scale of the individual leaf, the relevant regulating quantity is the stomatal resistance (R_{st}), which depends on the distribution and condition of stomata on the leaf surface. Landscape-level fluxes scale inversely with the canopy resistance (R_c), representing the bulk stomatal resistance to gas exchange exerted by all leaves in the canopy in aggregate. The canopy resistance therefore provides a key for predicting both carbon assimilation and transpiration fluxes from vegetated surfaces. The predictive power of many climate and mesoscale forecast models has been significantly enhanced by the incorporation of a simple representation of R_c into the model land-surface parameterization (Avissar and Pielke, 1991; Dickinson et al., 1991; Mascart et al., 1991; Randall et al., 1996).

Canopy resistance is often estimated by applying detailed mechanistic models of photosynthesis-stomatal response developed for individual leaves (e.g., Collatz et al., 1991, 1992), then scaling leaf responses to the canopy level using models of light penetration and leaf adaptation as functions of position within the canopy (e.g., Sellers et al., 1996). While this bottom-up scaling approach has proven effective in reproducing observed assimilation fluxes, it involves the specification of many species-dependent parameters and requires a computationally expensive iterative solution that can become numerically unstable under certain conditions (Baldocchi, 1994). The accuracy of such an approach depends on the validity and robustness of the assumed scaling principles, which are strongly non-linear (see review by Norman, 1993).

An alternative is to model the canopy response to its environment in bulk, neglecting the behavior of individual leaves. For many applications, there are compelling reasons to approach the problem in this way. McNaughton and Jarvis (1991) demonstrate that negative feedbacks develop within the canopy system that can cause the canopy to have a more stable behavior in the face of environmental fluctuations than would an isolated leaf. They show that transpiration rates become less sensitive to changes in atmospheric temperature and vapor pressure deficit (VPD) and more tightly coupled to incident light as scale increases from the leaf to canopy level. Canopy carbon assimilation rates also respond more conservatively (and linearly) to modifying factors in comparison with rates observed in individual leaves (Haxeltine and Prentice, 1996). Therefore, detailed models of stomatal response often may not provide additional accuracy in estimating stand-level fluxes. Furthermore, simple scaling techniques may neglect important feedback and system effects.

Here, we propose an approach to modeling canopy resistance that exploits the conservative nature of transpiration and photosynthetic processes occurring on the stand level. The fundamental quantity used in this technique is the canopy light-use efficiency (LUE, designated β), defined here as the ratio between the net canopy carbon assimilation rate (A_c) and the photosynthetically active radiation (PAR) absorbed by the canopy (APAR). LUE has been measured for many different plant species, and has been found to be fairly conservative within vegetation classes when the plants are unstressed. Because assimilation scaling effects are implicitly incorporated into stand-level measurements of LUE, β can provide a valuable constraint to canopy resistance modeling.

β-constrained models are particularly well-suited to application over large geographical regions because they are founded on a quantity that can be derived with reasonable accuracy from remote sensing: APAR (e.g., Kumar and Monteith, 1981; Daughtry et al., 1983; Steinmetz et al., 1990; Myneni et al., 1995a, b; Landsberg et al., 1997). β models typically require fewer equations, fewer tunable-parameter specifications, and fewer ground-based measurements than do scaled-leaf parameterizations. For these reasons, many recent models of global net primary production have been constructed upon principles of LUE (e.g., Potter et al., 1993; Ruimy et al., 1994; Prince and Goward, 1995).

Here we derive a simple, analytical expression for canopy resistance that is semi-constrained by field measurements of canopy LUE, averaged over broad vegetation categories. Despite its simplicity, this equation reproduces many of the subtle dependencies of LUE on environmental factors that are observed in nature. When embedded within the framework of a two-source (plant+soil) model of Atmosphere-Land Exchange (ALEX[1]), this equation provides hourly and daily estimates of evapotranspiration and carbon assimilation fluxes that agree well with micrometeorological measurements made in stands of corn,

[1] Source code available from M.C. Anderson.

soybean, prairie grasses, desert shrubs, rangeland, and black spruce.

2. Light-use efficiency

Numerous studies have demonstrated linearity in the relationship between the increase in canopy biomass during vegetative growth and the amount of visible light intercepted or absorbed by leaves in the canopy (Monteith, 1966, 1972; Puckridge and Donald, 1967; Duncan, 1971). Linear relationships are also observed between photosynthetic carbon uptake and radiation receipt by a canopy. While this relationship can be markedly non-linear for individual leaves, curvature decreases on the canopy level, presumably because a smaller fraction of leaf area is operating under light-saturated conditions (Hesketh and Baker, 1969). Haxeltine and Prentice (1996) demonstrate that the semi-mechanistic photosynthesis models of Collatz et al. (1991, 1992) will yield linear relationships between assimilation and light interception when integrated over the canopy if it is assumed that the canopy redistributes nitrogen content to achieve optimal photosynthetic functioning. Furthermore, there is some evidence to suggest that the slope of this linear relationship, the canopy LUE, may be fairly conservative within the major vegetation classes, perhaps as a result of natural selection (Field, 1991; Goetz and Prince, 1998a). This is intriguing, because conservative relationships in nature often facilitate simpler modeling strategies.

The conservative nature of LUE in carbon uptake, however, is sometimes difficult to ascertain from the literature due to the wide variety of definitions and measurement techniques that have been employed in different experiments (see discussion in Norman and Arkebauer, 1991; Gower et al., 1999). In brief, the difficulties arise because these experiments have not adopted a common definition of (a) 'light use' nor of (b) 'carbon uptake'. A definition of light use requires identifying a bandwidth (total solar versus PAR), a form of usage (absorption versus interception), and a medium for utilization (green versus living and dead vegetation; leaves, stems, branches, flowers or whole plant). Carbon uptake has alternately been defined as carbon fixed by photosynthesis (assimilation) or as biomass increment (above ground, or above+below ground). Often subtle mechanisms for biomass losses, such as herbivory, decomposition, and root sloughing, have been disregarded. Finally, an appropriate interpretation of light-use and carbon-uptake measurements depends on the measurement time and timescale (hour, day, day+night, season). For example, daytime measurements of LUE exclude night respiration costs and will thus overestimate multi-day averages.

For the purposes of studying net primary production in terrestrial ecosystems, Gower et al. (1999) compiled from the literature a list of LUE measurements based on annual or seasonal biomass accumulation for several major vegetation types and converted them to a common unit of grams total (above+below ground) net primary production per MJ APAR. APAR is the preferable definition of light use in this context because (a) photons in the PAR band are most intimately involved in the photosynthetic process, while NIR photons in the solar spectrum are predominantly reflected or scattered by the canopy; and (b) the fraction of incident PAR absorbed by green vegetation (f_{APAR}) is a quantity that can be remotely sensed as has been shown with both empirical (e.g., Daughtry et al., 1983; Steinmetz et al., 1990; Landsberg et al., 1997) and theoretical studies (e.g., Kumar and Monteith, 1981; Myneni et al., 1995a, b). Gower et al. (1999) prescribe the conversion process for different definitions of light use and carbon uptake used in the original papers.

For our purposes here, focussing on fluxes rather than productivity, we define LUE as 'the net carbon dioxide uptake by the canopy (intake less respiration, in moles) per mole PAR photons absorbed by green vegetation in the canopy.' Productivity estimates can be extracted if the conversion from moles carbon sequestered to grams dry matter is known. This conversion efficiency is species-specific and depends on the amount of carbon required to build carbohydrates, proteins and lipids and the relative amounts of these constituents within the plant tissues. Vertregt and Penning de Vries (1987) tabulate 'reciprocal glucose values' (GVI) for describing the energy content of dry matter for several different crops, and Griffin (1994) summarizes construction costs for several tree species. Conversion from LUE in g NPP (MJ APAR)$^{-1}$ to LUE in mol CO_2 (mol APAR)$^{-1}$ then is accomplished through

Table 1
Mean and standard deviations among measurements of LUE reported by Gower et al. (1999) for several major vegetation groups[a]

Vegetation group	*N*	Average LUE	Standard deviation in LUE
Agriculture — C_3	15	0.029	0.006
Agriculture — C_4	17	0.034	0.008
Agriculture — Nitrogen fixers	10	0.021	0.008
Boreal evergreen	4	0.007	0.001
Boreal deciduous	2	0.010	0.001
Temperate evergreen	15	0.006	0.003
Temperate deciduous	6	0.011	0.004
Tropical evergreen	13	0.012	0.008

[a] All LUE values have been converted to units of mol CO_2 mol^{-1} APAR from their original units of g NPP per MJ APAR using glucose content values from Vertregt and Penning de Vries (1987) and Griffin (1994). *N* indicates the number of LUE measurements used to compute the average and standard deviation for each vegetation group.

$$\begin{aligned}\mathrm{LUE}\left[\frac{\mathrm{mol\,CO_2}}{\mathrm{mol\,APAR}}\right] &= \mathrm{LUE}\left[\frac{\mathrm{g\,NPP}}{\mathrm{MJ\,APAR}}\right]\left[\frac{\mathrm{MJ\,APAR}}{4.6\,\mathrm{mol\,APAR}}\right] \times \mathrm{GVI}\left[\frac{\mathrm{g\,hexose}}{\mathrm{g\,NPP}}\right]\left[\frac{44\,\mathrm{g\,CO_2}}{30\,\mathrm{g\,hexose}}\right] \times \left[\frac{\mathrm{mol\,CO_2}}{44\,\mathrm{g\,CO_2}}\right] = 0.0072 \times \mathrm{GVI} \\ &\quad \times \mathrm{LUE}\left[\frac{\mathrm{g\,NPP}}{\mathrm{MJ\,APAR}}\right]. \qquad (1)\end{aligned}$$

Table 1 lists mean values and standard deviations of standardized LUE measurements reported by Gower et al. (1999) for several different vegetation groups, converted into units of mol CO_2 (mol APAR)$^{-1}$ using Eq. (1) (the grassland measurements in Gower et al. (1999) have been omitted here because information on light interception was not included in the original papers). When brought to a common standard, the conservative quality of LUE becomes more apparent (see also Fig. 6 of Gower et al., 1999).

Conservation of LUE is observed most prominently over an annual timescale. Over shorter timescales, there are several factors that will cause temporal variations in LUE. Seasonal cycles in the respiration to assimilation ratio for a given vegetation type will induce synchronized oscillations in net LUE. Evergreens, for example, spend a fraction of the year dormant while still collecting light; LUEs based on annual biomass accumulation will therefore underestimate production during peak growth periods. Because of variability in respiratory behavior between plant species, it is likely that gross LUE (reflecting gross CO_2 uptake), and not net LUE, is the truly conservative quantity (Goetz and Prince, 1998b). Gross LUE, however, is a difficult quantity to measure in practice, and respiration models are still required to infer NPP.

On still shorter timescales (daily and hourly), LUE can be influenced by an array of environmental factors, including extreme temperatures, soil moisture stress, nutrient limitations and high atmospheric VPDs (Runyon et al., 1994; Landsberg and Hingston, 1996). The variable partitioning of PAR incident above the canopy into direct beam and diffuse components (due to sun angle, clouds, etc.) can also affect LUE (Norman and Arkebauer, 1991). Diffuse light is more evenly distributed over leaves in the canopy, causing a smaller fraction of the leaves to operate in a light-saturated mode where photons are wasted. Carbon uptake efficiency in some conifers is particularly sensitive to diffuse lighting conditions, as needle photosynthesis can saturate at low quantum flux densities (Leverenz and Jarvis, 1979).

The LUE model as presented here responds to changes in light composition, soil moisture availability, ambient CO_2 concentration, and atmospheric demand; empirical temperature and nutrient response functions will be incorporated in future studies.

3. Model description

3.1. Analytical canopy resistance submodel

The conceptual structure of the ALEX model is diagrammed in Fig. 1 and is described in greater detail

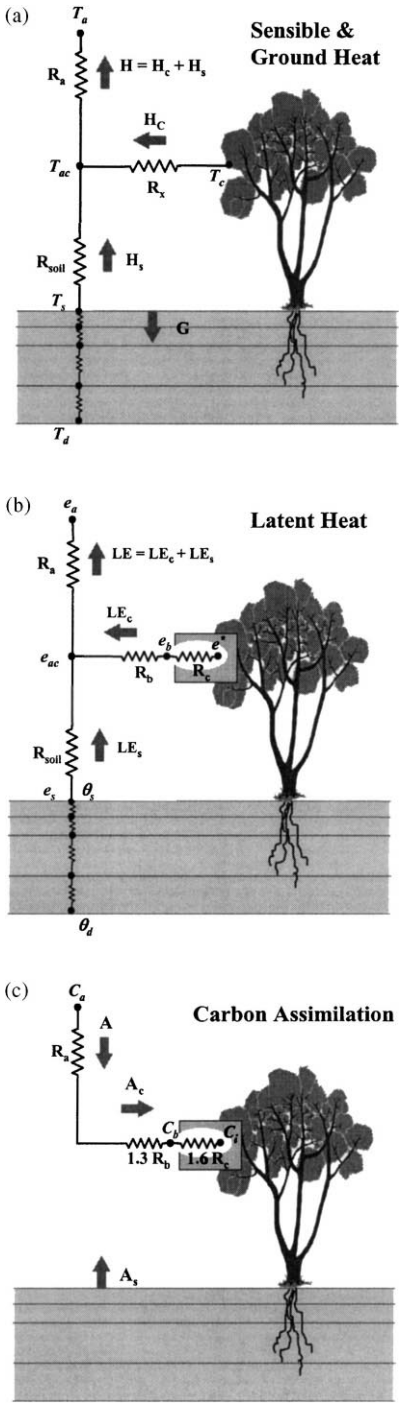

Fig. 1. Transport resistance networks used in the ALEX model to compute fluxes of (a) sensible and soil heating, (b) latent heating and (c) assimilated carbon.

in Appendix A; here we concentrate on the embedded analytical submodel for canopy resistance. In the following, the subscripts 'a', 'ac', 'b', and 'i' will refer, respectively, to bulk average conditions above the canopy, within the canopy air space, within the boundary layer at the leaf surface, and inside substomatal cavities (see Fig. 1). The subscript 'c' refers to fluxes and properties associated with the canopy in bulk, and 's' to conditions at the soil surface. Model state variables of temperature, vapor pressure, and carbon dioxide concentration are designated as T (K), e (kPa), and C (mol CO_2 mol^{-1}air), respectively.

The series–parallel resistance network used in Fig. 1 to define sensible and latent heating establishes feedback between soil and canopy fluxes and the in-canopy microclimate. Pathways for carbon transport from the soil and vegetation have been decoupled for computational simplicity; this is a reasonable approximation in most circumstances. Note that humidity and carbon concentration conditions at the leaf surface, within the laminar boundary layer, are modeled explicitly in this submodel; these layers can play an important role in mediating feedback loops that influence stomatal response on the canopy level (Collatz et al., 1991; McNaughton and Jarvis, 1991).

In Fig. 1, R_c and R_b are, respectively, the effective stomatal and boundary layer resistances to water vapor diffusion exerted by all leaves in the canopy in bulk, R_a is the aerodynamic resistance to turbulent transport between the canopy and the measurement reference height, and R_s is the resistance through the boundary layer above the soil surface. R_b is related to R_x, the total two-sided leaf boundary layer resistance integrated over all leaves in the canopy, as $R_b = (f_s/[f_g \times f_{dry}])R_x$. The factor f_s adjusts for a possible inequality in the distribution of stomata over the top and bottom sides of the leaf (f_s=1 for amphistomatous leaves, and 2 for hypostomatous leaves), the fraction of green vegetation in the canopy (f_g) excludes stomata on dead leaves from the net transport path, while the dry vegetation fraction (f_{dry}) excludes stomata blocked by liquid water on leaf surfaces, accumulated through precipitation or condensation (evaporative fluxes from the wet leaf area are treated in Appendix A). Forms used here for R_a, R_x and R_s are summarized by Kustas et al. (2000).

Given this transport framework, the following flux equations for canopy transpiration (LE_{ct}, defined as

positive away from the canopy in units of $W\,m^{-2}$) and net carbon assimilation (A_c, positive toward the canopy in units of $\mu mol\,m^{-2}\,s^{-1}$) can be written:

$$LE_{ct} = \lambda \frac{e_i - e_{ac}}{P(R_c + R_b)} \quad (2)$$

$$LE_{ct} = \lambda \frac{e_i - e_b}{PR_c} = \lambda \frac{e_i(1 - RH_b)}{PR_c} \quad (3)$$

$$A_c = \frac{C_a - C_i}{1.6R_c + 1.3R_b + R_a} \quad (4)$$

$$A_c = \frac{C_a - C_b}{1.3R_b + R_a} \quad (5)$$

where λ is the latent heat of vaporization in $J\,\mu mol^{-1}$, P is the atmospheric pressure in kPa, and resistances are in units of $m^2\,s\,\mu mol^{-1}$. The air within the stomatal pores is assumed to be saturated at the mean temperature of the canopy, T_c, so $e_i = e^*(T_c)$ and the relative humidity inside the leaf boundary layer $RH_b = e_b/e_i$. The resistance multipliers in the denominators of Eqs. (4) and (5) account for the relative diffusivities of CO_2 and water vapor.

Studies of gas exchange with isolated leaves subjected to varying environmental conditions have generated a family of simple empirical relationships between stomatal conductance and conditions at the leaf surface. Ball et al. (1987), for example, proposed the linear response function

$$\frac{1}{R_{st}} = b + m \frac{A_{leaf}\, RH_{b,leaf}}{C_{b,leaf}} \quad (6)$$

where R_{st}, A_{leaf}, $RH_{b,leaf}$ and $C_{b,leaf}$ refer to measurements made at the leaf-level. The coefficients b and m have been measured for several plant species and have been found to be fairly conservative within the C_3 and C_4 functional categories (Ball, 1988; Norman and Polley, 1989; Leuning, 1990; Collatz et al., 1991; Lloyd, 1991; Gutschick, 1996). A scaling from leaf to canopy level is effected by integrating in parallel over all dry, green leaf area (F_{dg}):

$$\frac{1}{R_c} = b_c + m \frac{A_c\, RH_b}{C_b} \quad (7)$$

where $b_c = b \times F_{dg}$, $F_{dg} = F \times f_{dry} \times f_g$, and F is the total leaf area index. The factor F_{dg} appears explicitly in the first term in Eq. (7) and implicitly in the second term in the bulk canopy values of A_c, RH_b and C_b.

It should be noted that many modified forms of the original Ball et al. (1987) stomatal response function (Eq. (6)) have appeared in the literature since its introduction (e.g., Leuning, 1990, 1995; Lloyd, 1991; Kustas et al., 2000). These modifications address some of the shortcomings of Eq. (6), including breakdown at very low light, humidity, and CO_2 levels. Furthermore, there is evidence to suggest that the primary variable driving stomatal response to humidity is not RH_b, but rather saturation VPD (Aphalo and Jarvis, 1991) or transpiration rate (Friend, 1991; Mott and Parkhurst, 1991; Monteith, 1995). Despite these objections, the very simple, linear form in Eq. (6) has proven reasonably effective over a range of environmental conditions. It is used here to minimize the number of tunable parameters required by ALEX and to facilitate an analytical solution for canopy resistance.

Given measurements or estimates of F, f_g, f_{dry}, C_a, R_b, R_a, e_{ac}, and $e_i = e^*(T_c)$ (in this case, e_{ac}, T_c and f_{dry}, are provided by the ALEX model, as described further), the unknowns in Eqs. (2)–(5) and (7) are R_c, A_c, LE_c, C_b, C_i, and RH_b. One more equation is required to close the system, and this equation must introduce the dependence of canopy resistance on the incident quantum flux density. Here we invoke the empirical observation that, in the absence of stress conditions, the rate of carbon assimilation by a canopy is nearly linearly proportional to the flux of photosynthetically active radiation absorbed by living vegetation in the canopy (APAR):

$$A_c = \beta\, \mathrm{APAR} \quad (8)$$

where β (mol CO_2 mol^{-1} quanta) is the canopy LUE.

Under optimal conditions, LUE is found to be relatively consistent across plant species within the C_3 and C_4 classes (see Table 1); however, as discussed earlier, canopy LUE will deviate from this nominal value in response to certain varying environmental conditions. To accommodate such modulating effects on assimilation rate, β has been cast as a function of the ratio of intercellular to ambient CO_2 concentrations ($\gamma = C_i/C_a$):

$$A_c = \beta(\gamma)\mathrm{APAR}. \quad (9)$$

The concentration of CO_2 within the substomatal cavities, C_i, is regulated by the relative rates of carbon supply through the stomata and fixation through the

photosynthetic process. Several studies have shown that γ is remarkably constant for leaves of a given species over a wide range of conditions, with typical values of 0.4 for C_4 plants and 0.6–0.8 for C_3 plants (Wong et al., 1979; Long and Hutchin, 1991). Conditions that cause this ratio to vary often affect the canopy LUE as well. For example, stomatal closure in response to a desiccating environment will tend to move the canopy toward a lower value of LUE, while simultaneously decreasing the average C_i through continuing fixation. An enhancement in the ratio of diffuse to direct-beam radiation (i.e., due to low sun angle or increased cloud cover) may increase both LUE and C_i, as photosynthetic light-use in the uppermost leaves in the canopy becomes unsaturated. In general, a positive relationship between, β and C_i is expected on a canopy level.

We assume that under unstressed conditions the canopy will tend to operate near a nominal LUE (β_n) with a nominal value of C_i/C_a (γ_n), both values being characteristic of the particular vegetation species. Although the functional dependence of A_c on C_i is curvilinear for individual leaves, simulations with the Cupid soil–plant–atmosphere model (Norman and Arkebauer, 1991) indicate the relationship becomes linearized on the canopy level. To facilitate a low-order analytical solution for R_c, we assume this relationship is approximately linear in the regime that most canopies will tend to operate:

$$\beta(\gamma) = \frac{\beta_n}{\gamma_n - \gamma_0}(\gamma - \gamma_0). \tag{10}$$

Typical values for the parameters β_n, γ_n and γ_0 for C_3 and C_4 canopies have been determined through numerical experimentation with the Cupid model assuming an ambient CO_2 concentration of 340 ppm (see Table 2). For C_4 plants, the offset γ_0 appears negligible; however, a significant positive offset is associated with C_3 canopies. These findings are consistent with the behavior of the CO_2 compensation points observed in C_3 and C_4 species (Collatz et al., 1991, 1992).

Eqs. (2)–(10) can be combined to yield a cubic function in R_c:

$$R_c^3 + C_1 R_c^2 + C_2 R_c + C_3 = 0 \tag{11}$$

where

$$C_1 = \frac{\alpha b_c - 1.6(1 - b_c R_b) + (1 - \gamma_0) m \frac{e_{ac}}{e_i}}{1.6 b_c}$$

$$C_2 = \frac{-\alpha(1 - b_c R_b) - 1.6 R_b + (1 - \gamma_0) m R_b}{1.6 b_c}$$

$$C_3 = \frac{-\alpha R_b}{1.6 b_c}$$

and

$$\alpha = \frac{C_a(\gamma_n - \gamma_0)}{\beta_n \mathrm{APAR}} + \gamma_0(1.3R_b + R_a)$$

$$R_2 = 1.3R_b + R_a.$$

The roots of Eq. (11) can be extracted analytically (see, e.g. Press et al., 1992); the positive root corresponds to a physical value for the canopy resistance. Given this estimate of R_c, canopy transpiration can be computed from Eq. (2), and assimilation by eliminating C_i from Eqs. (4) and (9):

$$A_c = \frac{C_a \beta_n \mathrm{APAR}(1 - \gamma_0)}{C_a(\gamma_n - \gamma_0) + \beta_n \mathrm{APAR}(1.6R_c + 1.3R_b + R_a)}. \tag{12}$$

The modeled canopy resistance in Eq. (11) responds to changes in light, humidity, CO_2 concentration, and moderate variations in leaf temperature (by modulating the substomatal saturation vapor pressure, e_i). Stomatal closure in response to water stress and extreme temperatures can be simulated through incorporation of empirical stress functions (see Section 3.4).

3.2. LUE response to diffuse light fraction

As discussed in Section 2, LUE is known to increase under more diffuse lighting conditions, where light is more uniformly and efficiently distributed over the canopy. Norman and Arkebauer (1991) modeled this phenomenon using the Cupid model and found a nearly linear response of LUE to the fraction of PAR that is diffuse (f_{dif}). If 50% beam radiation is used as a reference, instantaneous values of the LUE for corn (C_4) may be 15% higher for diffuse light and 15% lower for a clear sky; however, for soybean (C_3), the variation may be ±40%. The difference in slope is due to the fact that C_3 canopies saturate at lower light levels than C_4 canopies.

Table 2
Input quantities required by the ALEX model and values used in model simulations

Quantity	ID	Units	Prairie	Rangeland	Soybean	Corn	Black spruce	Desert shrub
Experiment			FIFE '87	GEWEX/GCIP	GEWEX/GCIP	GEWEX/GCIP	BOREAS '96	MONSOON '90
Date			May–October 1987	June–July 1997	July–August 1998	July 1999	July 1996	July–August 1990
System								
Wind	u	$m\,s^{-1}$						
Air temperature	T_a	K						
Vapor pressure	e_a	kPa						
Atmospheric pressure	P	kPa						
Solar radiation	S_d	$W\,m^{-2}$						
Precipitation	W_0	mm						
Ambient CO_2 concentration	C_a	$\mu mol\,mol^{-1}$	340	340	340	340	340	340
Canopy								
Leaf area index	F	$m\,m^{-1}$	0.1–3.2	2.0–3.0	1.0–6.8	5.5–5.0	5.7	0.5
Canopy height	h_c	m	0.3–0.5	0.6	0.2–0.5	2.3	10.0	0.5
Clumping factor	Ω_c		1.0	1.0	1.0	1.0	0.5	0.7
Surface roughness	Z_m	m	$0.05\times h_c$	$0.05\times h_c$	$0.1\times h_c$	$0.1\times h_c$	$0.1\times h_c$	$0.16\times h_c$
Displacement height	d	m	$0.67\times h_c$	$0.67\times h_c$	$0.67\times h_c$	$0.67\times h_c$	$0.67\times h_c$	$0.44\times h_c$
Average leaf size	s	m	0.01	0.01	0.03	0.10	0.05	0.01
Fraction of green vegetation	f_g		0.1–1.0	1.0	1.0	1.0	1.0	0.8
Nominal LUE	β_n	$mol\,mol^{-1}$	0.03	0.02	0.025	0.04	0.007	0.02
Nominal C_i/C_a fraction	γ_n	$mol\,mol^{-1}$	0.6	0.8	0.8	0.6	0.8	0.8
C_i/C_a at $\beta=0$	γ_0	$mol\,mol^{-1}$	0.0	0.2	0.2	0.0	0.2	0.2
Ball & Berry slope	m		4.0	9.0	9.0	4.0	9.0	11.0
Ball & Berry offset	b	$\mu mol\,m^{-2}\,s^{-1}$	0.04×10^6	0.01×10^6	0.01×10^6	0.04×10^6	0.01×10^6	0.01×10^6
Minimum RH_b in Ball & Berry	$RH_{b,min}$		0.1	0.1	0.1	0.1	0.1	0.6
Leaf absorptivity (vis)	$\alpha_{leaf,v}$		0.80	0.80	0.85	0.85	0.88	0.85
Leaf absorptivity (NIR)	$\alpha_{leaf,n}$		0.15	0.15	0.15	0.15	0.55	0.15
Leaf absorptivity (TIR)	$\alpha_{leaf,l}$		0.97	0.97	0.97	0.97	0.97	0.97
Maximum interception	$W_{i\,max}$	mm	0.15	0.15	0.15	0.15	0.15	0.15
Maximum fraction of wetted leaf area	$f_{wet\,max}$		0.2	0.2	0.2	0.2	0.2	0.2
Rooting depth	d_r	m	2	2	2	2	1.5	2
Root density coefficient	τ		2.4	2.4	2.4	2.4	2.4	2.4
Soil								
Bulk density	BD	$g\,cm^{-3}$	1.15	1.5	1.5	1.5	1.3	1.35
Moisture release parameter	b_s		6.3	5.5	6.0	6.0	7.6	4.35
Air entry potential	ψ_e	$J\,kg^{-1}$	−1.2	−2.6	−2.1	−2.1	−3.7	−1.1
Saturated hydraulic conductivity	K_s	$kg\,s\,m^{-3}$	7.4×10^{-4}	4.0×10^{-4}	4.0×10^{-4}	4.0×10^{-4}	1.7×10^{-3}	1.0×10^{-3}
Soil emissivity	ε_s		0.96	0.96	0.96	0.96	0.96	0.96
Soil reflectivity (vis)	ρ_{sv}		0.15	0.15	0.15	0.15	0.15	0.15
Soil reflectivity (NIR)	ρ_{sn}		0.25	0.25	0.25	0.25	0.25	0.25
Surface ponding capacity	h_{max}	mm	5.0	5.0	5.0	5.0	5.0	5.0
Deep soil water content	θ_d	$m^3\,m^{-3}$	0.23	0.20	0.40	0.40	0.30	0.20
Deep soil temperature	T_d	K	298	298	278	278	274	293

To capture this response in hourly assimilation estimates, it is possible to modify the nominal LUE, β_n in Eq. (10) according to

$$\beta_n' = \beta_n \times [1 + 2\Delta_{dif}(f_{dif} - 0.5)] \quad (13)$$

where Δ_{dif}=0.4 for C_3 plants and Δ_{dif}=0.15 for C_4. If only daily-integrated fluxes are of interest, β_n can be left unmodified.

3.3. Temporal considerations — nighttime and seasonal fluxes

The appropriate averaging timescale for evaluating carbon flux estimates using Eq. (11) will depend on the timescale over which the LUE factor was measured. Flux estimates will be most accurate when the averaging and measurement timescales are commensurate.

If β_n was derived from daytime measurements of A_c versus APAR during a particular growth stage, Eq. (11) should provide reasonable hourly daytime flux estimates for that same growth stage. In this case, nighttime respiration flux can be estimated with an empirical function of canopy temperature.

If β_n was derived from seasonal dry matter accumulation measurements, Eq. (11) will give good estimates of seasonal NPP, but will underestimate daytime fluxes because nighttime respiration costs have been rolled into the LUE measurement. The degree of underestimation will depend on the ratio of respiration to net assimilation for each particular plant species. For black spruce, autotrophic respiration is approximately 60–70% of the gross primary production on an annual basis (Ryan et al., 1997), so the bias in this case would be large. With NPP-based LUE measurements, it is appropriate to set nighttime values of modeled A_c to zero, so that seasonally-integrated carbon flux estimates will be unbiased. With a seasonal and/or daily model of the respiration to assimilation ratio, it should be possible to unfold the nighttime respiration costs from β_n and obtain less biased estimates of net assimilation on shorter timescales.

3.4. Stress modification of canopy resistance

The fluxes LE_{ct} and A_c should be considered the potential fluxes that the canopy could attain in the absence of vegetative stress. Limiting plant-available water ('aw'), nutrients ('n'), or extreme temperatures ('t') can induce stomatal closure and reduce canopy fluxes below these potential levels. Following Jarvis (1976), stomatal response to stress on the canopy level is captured in ALEX through imposition of independent stress functionals:

$$R_c' = R_c \times f_{aw} \times f_t \times f_n \times \cdots \quad (14)$$

where R_c' and R_c are stressed and unstressed (from Eq. (11)) estimates of canopy resistance, respectively.

Studies investigating stomatal response to changes in various water status indicators typically show that stomatal conductance remains at a maximum (potential) level until the indicator drops below some threshold, at which point conductance decreases rapidly toward zero. Often the indicator used is leaf water potential, but a direct response to soil water potential has also been demonstrated (Gollan et al., 1986). A soil-water-based stress functional affords a much simpler overall modeling strategy, because leaf water potential depends on both soil moisture status and atmospheric demand.

Campbell and Norman (1998) outline a simple supply/demand-based scheme that relates depletion of the fraction of plant-available water in the root zone:

$$A_w = \frac{\theta - \theta_{pwp}}{\theta_{fc} - \theta_{pwp}} \quad (15)$$

to reductions in transpiration due to stomatal closure:

$$f_{aw} = 1 - \tfrac{2}{3}\left[A_w\left(0.03^{-1/b_s} - 1.5^{-1/b_s}\right) + 1.5^{-1/b_s}\right]^{-b_s} \quad (16)$$

where θ, θ_{fc}, θ_{pwp} are, respectively, the actual volumetric soil water content, and the water contents at field capacity and permanent wilting, and b_s is the exponent in the soil moisture release curve. Soil-water-limited transpiration and assimilation rates can then be approximated as

$$LE_{ct}' = f_{aw} \times LE_{ct} \quad (17)$$

$$A_c' = f_{aw} \times A_c \quad (18)$$

where the potential fluxes LE_{ct} and A_c have been computed neglecting soil water effects as described in Section 3.1. Under this scheme, plants transpire and

photosynthesize at nearly their potential rate until they have extracted about half the available water from the root zone; further extraction takes an increasing toll on these exchanges.

Several generic temperature response functions are available in the literature; frequently, simply specifying species-dependent upper and lower temperature cutoffs for photosynthetic uptake is sufficient. The effects of extreme temperatures are neglected in the simulation studies presented below because the modeled canopy temperatures were typically within ranges considered optimal for photosynthesis.

3.5. ALEX: A coupled canopy resistance–energy balance model

The field measurements required by the canopy resistance submodel described in Section 3.1 are minimal: above-canopy wind speed (for R_a and R_b) and CO_2 concentration (C_a), canopy leaf area index (F) and fraction of green vegetation (f_g), approximate leaf size (s), canopy height (for estimates of surface roughness and displacement height), and PAR absorbed by green vegetation (APAR). APAR can be estimated from remote sensing information, or from a model of radiative transfer through a canopy. A simple analytical form for APAR depending on solar irradiance, LAI, leaf angle distribution, leaf absorptivity and soil reflectance is outlined in Appendix B.

Estimates of bulk canopy temperature (T_c, for computing e_i) and in-canopy vapor pressure (e_{ac}) are also required; here, these inputs are supplied by coupling the canopy resistance equation (Eq. (11)) with a canopy energy balance submodel. The resultant ALEX model is described in Appendix A; the complete set of inputs required by ALEX is listed in Table 2. ALEX also models the evolution of soil moisture content used in evaluating water stress effects on canopy resistance (Section 3.4), and estimates the rate of evaporation of standing water intercepted or accumulated by the canopy, providing a time-dependent estimate of f_{dry}.

4. Model validation

The accuracy of the coupled system of canopy resistance and energy balance equations comprising the ALEX model has been tested in comparison with micrometeorological measurements made in a variety of natural and agricultural ecosystems. These systems encompass a range in climatic regimes and plant species within both C_3 and C_4 functional groups, and thus constitute a useful test of the generality of this simple modeling strategy.

The ALEX model has also been compared with a significantly more detailed soil–plant–atmosphere model, Cupid (Norman, 1979; Norman and Campbell, 1983; Norman and Polley, 1989; Norman and Arkebauer, 1991). Cupid models the leaf-level responses of photosynthesis (using the formalism of Collatz et al., 1991, 1992, for C_3 and C_4 species, respectively) and energy balance to environmental forcings within multiple leaf classes, stratified by leaf angle and depth within the canopy. Canopy-level responses are simulated by numerical integration over all leaf classes. Because the Cupid and ALEX models share a common soil transport submodel, comparisons between Cupid and ALEX effectively evaluate the performance of the simplified top-down canopy-scaling approach taken in ALEX with respect to more detailed scaled-leaf modeling strategies.

4.1. Validation datasets

Energy and carbon flux measurements for model validation have been compiled from a variety of field experiments conducted across the US and Canada. Model inputs describing each site are listed in Table 2. Among these sites, the following vegetative regimes are represented:

(a) *Tallgrass prairie*: The First ISLSCP (International Satellite Land Surface Climatology Project) Field Experiment of 1987 (FIFE; Sellers et al., 1992) was conducted near the Konza Prairie Research Natural Area outside of Manhattan, KS. The flux measurements examined in this study were collected at FIFE Site 11 (Grid ID 4439); this site and the experimental procedures employed there are described in detail by Kim and Verma (1990a, b). The predominant soil type at this site was a Dwight silty clay loam, and the vegetation primarily warm season C_4 grasses such as big bluestem (*Andropogon gerardii*), indiangrass (*Sorghastrum nutans*), and switchgrass (*Panicum virgatum*).

The measurements used here were collected during each of the four 1987 Intensive Field Campaigns (IFCs), spanning the months of May through October and encompassing all the major phenological stages of the native prairie development. A severe dry-down occurred in July and into early August (IFC 3), significantly depressing carbon fluxes during this period (see Kim and Verma, 1990a). Leaf area index, soil moisture, and other input data required by the ALEX model were obtained from the FIFE CD-ROM data collection (Strebel et al., 1994). Anderson et al. (1997) outline the methodology used to estimate the fraction of green vegetation from measurements of live and dead plant dry weight collected throughout the experiment.

(b) *Rangeland grasses*: These measurements were collected at a flux facility operated by the National Oceanographic and Atmospheric Administration (NOAA), located in the Little Washita watershed in southwestern Oklahoma. This station was established as part of the GEWEX (Global Energy and Water Cycle Experiment) Continental-scale International Project (GCIP) centered on the Mississippi River Basin (Lawford, 1999). The Little Washita site occupies range- and pasture-land containing a mixture of C_4 grass species and C_3 weeds. The soil has been classified as clay loam. The pasture just outside the instrumentation enclosure has been grazed, which may account for the high degree of soil compaction reflected in the measured bulk density of $1.6\,g\,cm^{-3}$.

The data presented further were collected in June–July 1997. Available soil water appeared adequate to sustain high canopy transpiration and assimilation rates, and grasses were predominantly green during this period. Leaf area index was measured in mid-June at several locations around the flux station and was found to be quite variable due to grazing activity. The effective flux footprint will therefore depend to some extent on wind direction, so use of an average LAI value will unavoidably introduce some error into model flux estimates.

(c) *Agricultural — soybean and corn*: NOAA operates a second flux station under the GEWEX/GCIP program on a farm south of Champaign, IL (Baldocchi and Meyers, 1998). Production on the field surrounding this station rotates yearly between corn (*Zea maize*, C_4) and soybeans (*Glycine max*, C_3), and has been under no-till management since 1986. The soil is a silt loam.

The measurements examined here were obtained during the 1998 (soybean) and 1999 (corn) growing seasons in July and August. Local meteorological conditions in 1999 were prime for agriculture, with ample rainfall and sunshine, resulting in impressive carbon flux measurements in the corn stand.

(d) *Black spruce*: The Boreal Ecosystem–Atmosphere Study (BOREAS; Sellers et al., 1995) was undertaken to study carbon exchange with boreal forest ecosystems. Here we examine measurements acquired at the Old Black Spruce flux tower site in the BOREAS Northern Study Area, located in central Manitoba (Goulden et al., 1997; Sutton et al., 1998). Vegetation around the tower was predominantly 120-year-old black spruce (*Picea mariana*), with an underlying carpet of feather and sphagnum moss.

The flux measurements studied here were acquired during July 1996 with an eddy correlation system mounted above the forest canopy on a 31 m tower. The carbon eddy flux measurements were corrected for storage within the forest canopy, estimated as the time change in CO_2 concentration measured below the correlation system between hourly sampling times (Goulden et al., 1997). Energy fluxes were not corrected for in-canopy storage.

(e) *Desert shrubs*: Energy and water flux behavior in a semiarid rangeland ecosystem were studied in the MONSOON ’90 field experiment (Kustas and Goodrich, 1994), conducted in the Walnut Gulch Watershed in southern Arizona. The data examined here were collected in a shrub-dominated subwatershed in the Lucky Hills study area. This site is sparsely vegetated (F=0.5) with a variety of C_3 desert shrubs, including desert zinnia (*Zinnia pumlia*), white thorn (*Acacia constricta*), creosote bush (*Larrea tridentata*), and tarbush (*Florensia cernua*). The soil has been classified as a very gravelly sandy loam.

The measurements presented below were collected during the July–August field campaign, which coincided with the beginning of the ‘monsoon season’ in this region. Several large rainfall events occurred during this interval, interspersed with days of low humidity down to 15–20%.

While carbon fluxes were not monitored at this site, several measurements were taken specifically for testing canopy/soil partitioning algorithms. Thermodynamic temperatures of representative canopy and soil components near the flux system were measured

periodically with infrared thermometers (Norman et al., 1995). In addition, system latent heat flux measurements were partitioned into soil and canopy contributions using a chamber measurement technique described by Stannard (1988).

4.1.1. Energy budget closure corrections

Each of the flux datasets listed earlier was acquired using the eddy covariance measurement technique, which does not enforce closure among energy flux components. Possible causes for non-closure include errors in the measurement of net radiation and/or soil heat flux, unaccounted heat storage within the canopy (including photosynthesis), and non-stationary or dispersive eddy components that are not sampled by the covariance system. The datasets listed earlier have average closure errors on the order of 10–20% of the measured net radiation.

For comparison with flux estimates from the ALEX model, where energy closure is enforced, the eddy flux measurements were corrected for closure errors using a strategy suggested by Twine (1998) and others. The observed values of H and LE were modified such that they summed to the available energy ($RN-G$) yet retained the observed Bowen ratio. Twine (1998) tested several closure correction strategies and found this technique yielded best agreement between eddy correlation and Bowen ratio flux measurements taken during the Southern Great Plains Experiment of 1997 (SGP '97; Jackson, 1997). This correction was not applied to the black spruce flux database, as energy storage within the forest canopy may have been significant.

4.1.2. Soil respiration corrections

Carbon flux measurements on the stand level typically sample the net ecosystem CO_2 exchange (A), which incorporates contributions from the soil, roots and groundcover (A_s; defined as positive away from the soil surface as in Fig. 1) as well as the canopy uptake (A_c):

$$A = A_c - A_s \tag{13}$$

To isolate A_c for comparison with model predictions, the soil component must be added to the system measurement.

For the black spruce dataset, an empirical function of soil temperature developed in situ by Goulden and Crill (1997) was used to estimate A_s, including contributions from moss respiration. For the other datasets, A_s was modeled using an empirical relationship developed by Norman et al. (1992) in a site within the FIFE experimental area, depending on soil temperature and moisture content and LAI (a surrogate for root density). This relationship also provides reasonable estimates of soil fluxes measured in prairie and corn in Wisconsin (Wagai et al., 1998), but may need adjustment for other ecosystems.

4.2. Canopy/soil partitioning

The canopy resistance submodel developed in Section 3 requires estimates of canopy temperature and humidity, generated in this application by the energy-partitioning component of the ALEX model. To verify that this component behaves reasonably, we have utilized soil and canopy state and flux measurements made during the MONSOON '90 field experiment.

Kustas et al. (2000) used this dataset to evaluate the performance of the Cupid soil–plant–atmosphere model under semiarid climatic conditions. They found that reasonable agreement between modeled and measured fluxes could be obtained with a minor modification to the Ball et al. (1987) stomatal response function, which in effect reduces the influence of leaf-surface relative humidity when it falls below some threshold value $RH_{b,min}$. This modification remedies the well-known failure of the Ball et al. (1987) function at low humidities, which were prevalent during the MONSOON '90 campaign. Because the non-linear correction function suggested by Kustas et al. (2000) (their Eq. (4)) would increase the order of an analytical solution for R_c, a linear approximation has been implemented in ALEX: the value of RH_b used in Eq. (7) is fixed at $RH_{b,min}$ for solutions that yield $RH_b < RH_{b,min}$.

Estimates of the primary flux components from the ALEX model are compared with hourly measurements from MONSOON '90 in Fig. 2 (see Table 3 for statistical details). The level of agreement here is similar to that achieved by the more significantly detailed Cupid model (see Kustas et al., 2000). Enforcement of closure among the eddy covariance measurements

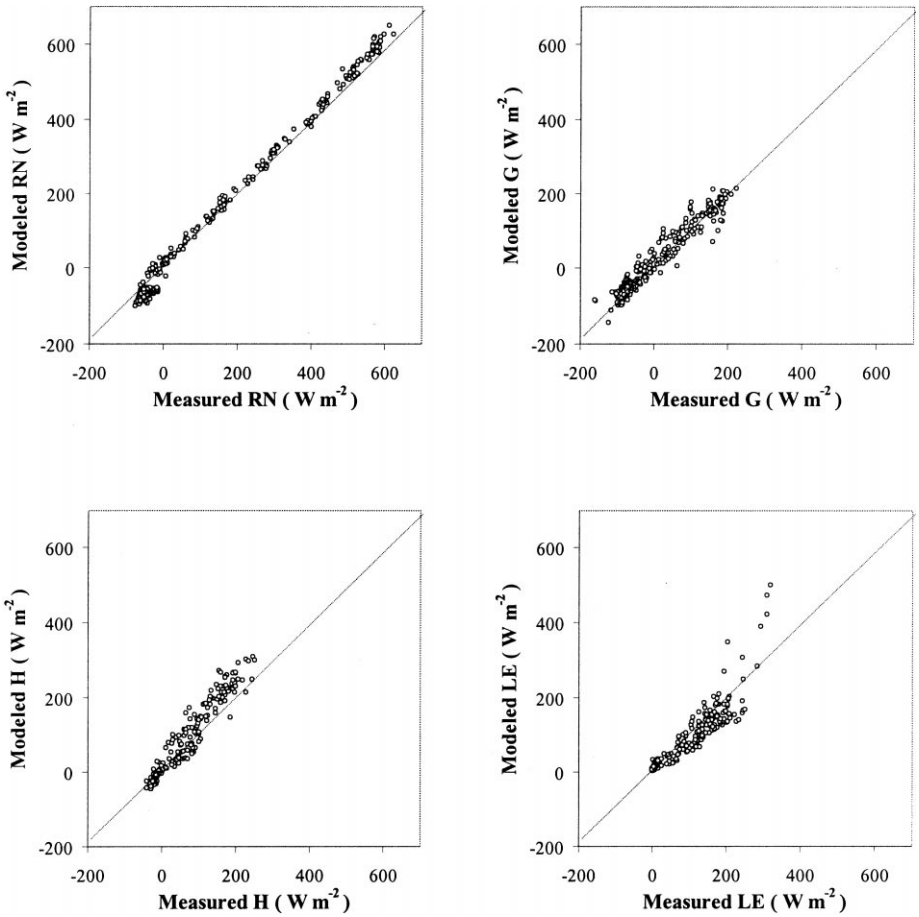

Fig. 2. Comparison of primary energy flux component measurements made during MONSOON '90 with estimates from the ALEX model.

improves the agreement with both models. Comparisons between ALEX predictions of canopy and soil temperature and evaporation and measurements are contained in Fig. 3. Here, the component evaporation measurements have been adjusted such that they sum to the closure-corrected system evaporation flux while maintaining the measured soil/canopy partitioning ratio. Again, the performance is similar to that of Cupid; both show a tendency to under-predict transpiration, perhaps due to residual problems with the modified Ball et al. (1987) at low humidities.

4.3. Canopy resistance and light-use efficiency

Canopy resistance estimates from ALEX and Cupid simulations, using meteorological inputs from FIFE '87, are compared in Fig. 4. In Cupid, R_c is computed as a leaf-area-weighted summation of $R_{s,leaf}$ over all leaf angle and layer classes in the canopy. The analytical model for R_c developed here produces values that agree well with those derived numerically by Cupid. Note that the dry-down that occurred during the 3rd IFC ($f_{aw}<0.5$) effected significant stomatal closure in both models.

Fig. 5 demonstrates the ability of the analytical model to reproduce observed diurnal patterns in LUE response to variations in VPD and direct versus diffuse incident PAR. These are eight consecutive days of measurements made in corn in Champaign, IL during 1999. Post-dawn and pre-dusk enhancements in the observed LUE, corresponding with times when irradiation is highly diffuse

and VPD is low, are also found in the modeled efficiencies.

4.4. Carbon and evapotranspiration fluxes

Carbon assimilation and evapotranspiration fluxes simulated with the ALEX model, using inputs listed in Table 2, are compared with hourly eddy covariance measurements in Fig. 6; Table 3 provides a statistical description of these compansons. Included here are the root-mean-square-difference (RMSD), and the daytime mean-absolute-percent-difference ($MAPD_{day}$), defined as the absolute value of the difference between predicted and observed flux divided by the observed flux, multiplied by 100. Because this statistic is ill-behaved as the observed quantity approaches zero, we include only fluxes when $RN>100\,W\,m^{-2}$ in the computation of $MAPD_{day}$.

Table 3
Quantitative measures of model performance in estimating hourly carbon and heat fluxes[a]

Flux	Cover	N	O	S_o	RMSD	MBE	a	b	R^2	$MAPD_{day}$
A_c	Prairie	544	17.2	10.0	3.6	−0.6	1.3	0.89	0.87	24
	Rangeland	1085	13.2	6.8	3.1	−1.1	1.7	0.79	0.82	33
	Soybean	1573	16.7	8.9	4.9	−0.2	1.8	0.88	0.73	35
	Corn	811	33.2	19.6	7.6	1.1	6.5	0.84	0.85	20
	Black Spruce	833	6.3	4.2	3.6	−2.3	1.4	0.42	0.64	48
	All	4846	17.0	13.4	4.8	−0.6	0.4	0.94	0.88	33
RN	Prairie	851	255	240	49	24	−10	1.13	0.99	12
	Rangeland	1920	176	241	29	−5	−22	1.09	0.99	6
	Soybean	2974	139	199	36	−1	−20	1.14	0.99	11
	Corn	1440	154	238	25	5	−2	1.04	0.99	7
	Black Spruce	1284	160	226	30	−16	−21	1.03	0.99	6
	Desert Shrub	336	136	226	22	−7	−14	1.05	0.99	4
	All	8805	164	227	33	−1	−16	1.09	0.99	9
LE	Prairie	721	167	142	45	8	21	0.92	0.91	20
	Rangeland	1907	123	141	33	−7	4	0.91	0.95	16
	Soybean	2873	117	146	34	−5	−1	0.96	0.95	19
	Corn	1389	133	166	32	0	2	0.98	0.96	15
	Black Spruce	1262	48	59	31	9	18	0.80	0.74	62
	Desert Shrub	199	108	81	43	−19	−4	0.86	0.78	27
	All	8351	115	141	34	−2	4	0.95	0.94	24
H	Prairie	721	55	89	43	10	8	1.03	0.83	91
	Rangeland	1907	31	70	35	17	20	0.90	0.82	135
	Soybean	2873	18	41	26	4	7	0.81	0.66	167
	Corn	1389	2	59	30	−2	8	0.63	0.77	126
	Black Spruce	1283	78	139	67	−5	−10	1.06	0.83	154
	Desert Shrub	199	69	80	40	21	0	1.31	0.95	41
	All	8372	36	81	39	5	7	0.97	0.80	138
G	Prairie	829	25	42	42	5	−7	1.46	0.73	181
	Rangeland	1920	16	44	41	−10	−19	1.56	0.82	155
	Soybean	2974	5	28	40	2	−1	1.50	0.55	420
	Corn	1440	5	26	34	2	−1	1.66	0.70	319
	Desert Shrub	336	0	96	24	9	9	0.92	0.95	41
	All	7499	10	40	39	−1	−4	1.35	0.69	279

[a] Here N is the number of observations, O and S_o are the mean and standard deviations of the observations, RMSD is the root-mean-square-difference between the modeled (P) and observed (O) quantities, MBE is the mean-bias-error, a and b are the intercept and slope of the linear regression of P on O, R^2 is the coefficient of determination, and $MAPD_{day}$ is the mean-absolute-percent-difference between daytime observations and model predictions. The terms N, b, $R^2$and $MAPD_{day}$ are unitless; O, S_o, RMSD, MBE, and a have units of $\mu mol\,m^{-2}\,s^{-1}$ for A_c and units of Wm^{-2} for *RN*, *LE*, *H* and *G*.

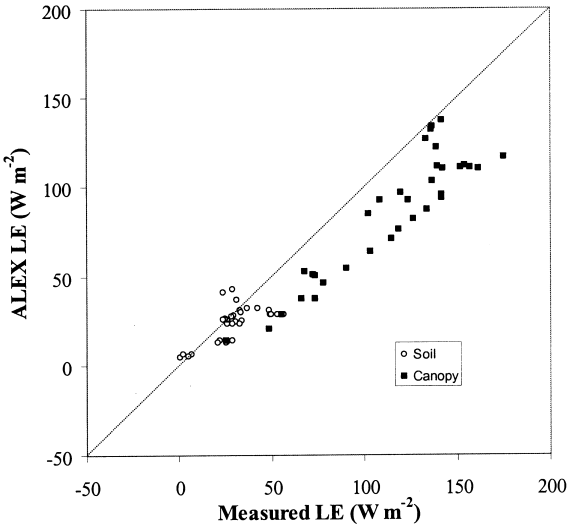

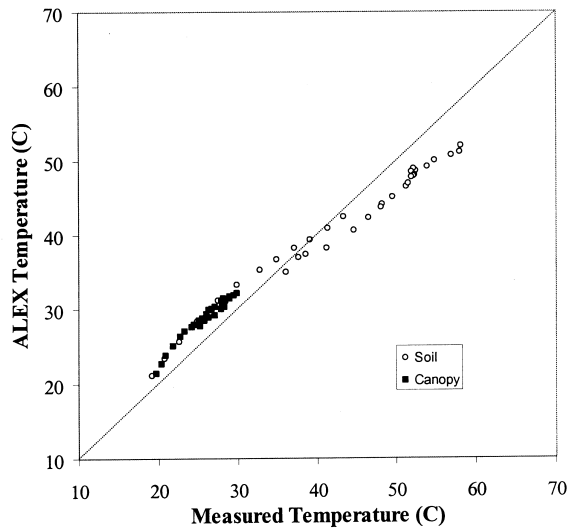

Fig. 3. Comparison of predicted soil-surface and vegetation evaporation rates and temperatures with measurements from MONSOON '90.

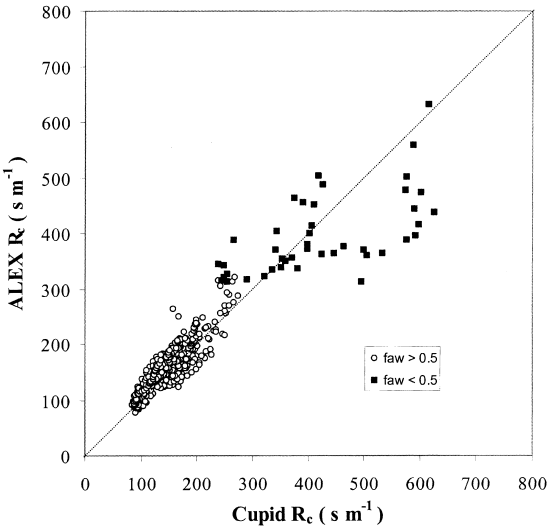

Fig. 4. Comparison of canopy resistance values predicted by the ALEX and Cupid models for flux measurements obtained during FIFE '87.

Hourly carbon flux comparisons in Fig. 6 and Table 3 have been restricted to daytime hours (solar irradiation $> 50\ \mu mol\ m^{-2}\ s^{-1}$), while comparisons of latent heat fluxes include day and nighttime measurements.

As evident in Fig. 6, the analytical canopy resistance submodel in ALEX does reasonably well at reproducing measured carbon and water fluxes on an hourly timescale. Its success is particularly notable given the simplicity of the model and the limited number of tunable parameters it requires. The measurements displayed here represent a wide range in atmospheric, soil moisture, and phenological conditions. The effects of stomatal closure during the dry-down in the 3rd FIFE IFC, for example, are well-reproduced by the soil moisture stress term (f_{aw}, Eq. (16)). During this interval, f_{aw} varied between 0.4 and 0.9. If soil moisture effects are ignored during this IFC, A_c is overestimated by up to $25\ \mu mol\ m^{-2}\ s^{-1}$, and LE by $250\ W\ m^{-2}$.

The $MAPD_{day}$ statistic in Table 3 permits comparison of model errors with typical uncertainties associated with micrometeorological measurement techniques. Kustas and Norman (1997) summarize results of intercomparisons of flux measurement techniques made during FIFE '87 and '89 (Nie et al., 1992; Fritschen et al., 1992). On an hourly or half-hourly basis, measurements of daytime latent and sensible heating made with several eddy correlation and Bowen ratio systems typically differed by 20–30%. After normalization of net radiation measurements to a roving radiometer standard and enforcement of energy closure, Twine (1998) found instrumental variations of 5, 10 and 20% for hourly measurements of daytime net radiation, latent and sensible heat, respectively, made during SGP '97. Eddy correlation

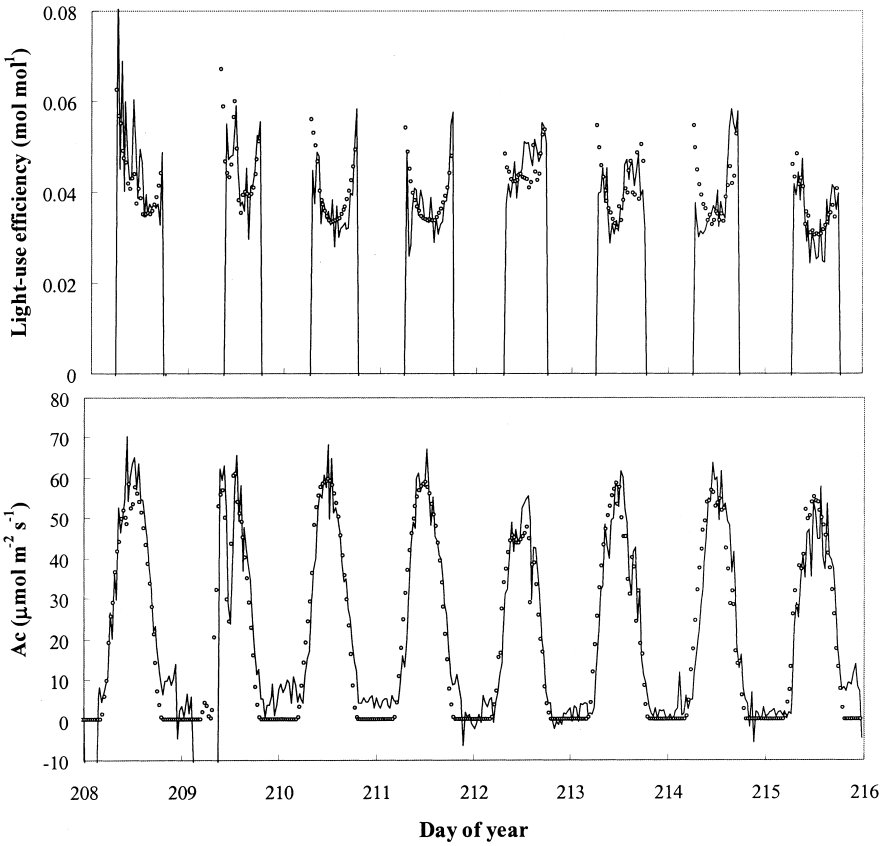

Fig. 5. A time-course of measurements of effective light-use efficiency and carbon assimilation measurements made in corn over eight consecutive days (lines). Also plotted are simulated values of LUE and A_c generated by the ALEX model (circles).

carbon flux systems used during FIFE '89 showed 5–15% variations (Moncrieff et al., 1992).

In comparison, the $MAPD_{day}$ values for hourly daytime flux estimates from the ALEX model, averaged over the six datasets represented in Table 3, are 9% (*RN*), 24% (*LE*), and 33% (A_c). The errors in *RN* and *LE* are comparable to observational errors encountered during FIFE. While the model RMSD for A_c is significantly larger than the expected error, the R^2 value of 0.88 is encouraging. Some of the scatter in the canopy assimilation comparisons is introduced by the empirical soil respiration correction to measured system carbon fluxes. Other important sources of error include inaccurate specification of green leaf area, and the use of a net LUE based on seasonal NPP measurements (see further).

Sensible and soil heating fluxes are less accurately determined from a MAPD standpoint. While the RMSD for all energy flux components is roughly equal on average (35–40 $W m^{-2}$), the low average magnitudes of *H* and *G* lead to high $MAPD_{day}$ values of 138 and 279%, respectively. The amplitude of the diurnal soil heat flux curve is consistently overestimated by ALEX, with the exception of the MONSOON '90 database. A calibration in sand of 14 different commercially-available soil heat flux plates conducted by Twine (1998) revealed that the plates consistently under-measured the known flux under both saturated and dry conditions. Translated to thermal conductivities typical of the FIFE site, for example, the expected bias is on the order of 5%. This may explain in part the disagreement between the modeled and measured diurnal soil flux amplitudes. In the ALEX formulation, H_c and H_s are essentially computed as residuals to the soil and canopy energy budgets, so any errors in the modeled

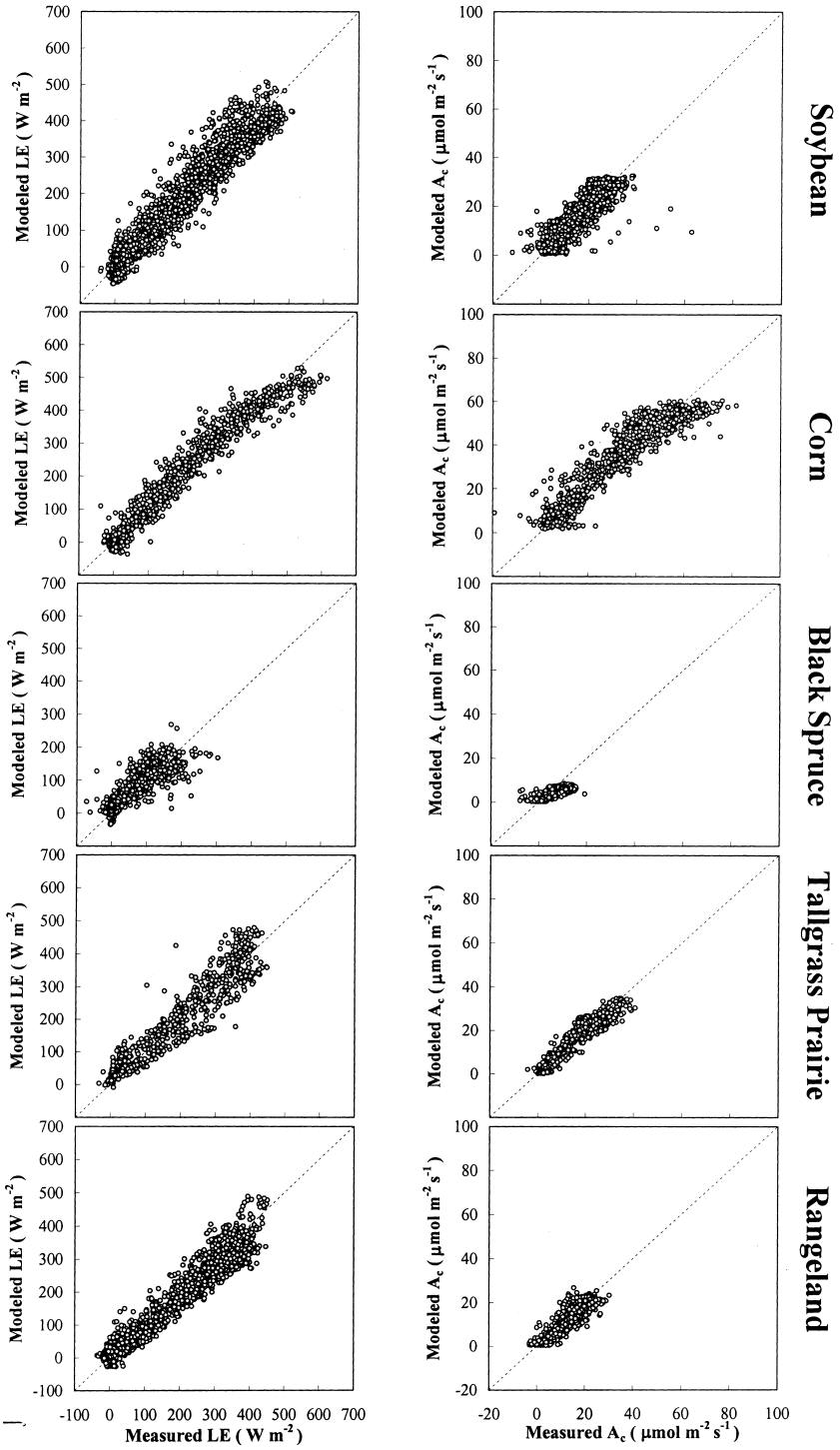

Fig. 6. Comparison of hourly measurements of system latent heating and canopy carbon assimilation made in five different vegetative stands with estimates generated by the ALEX model.

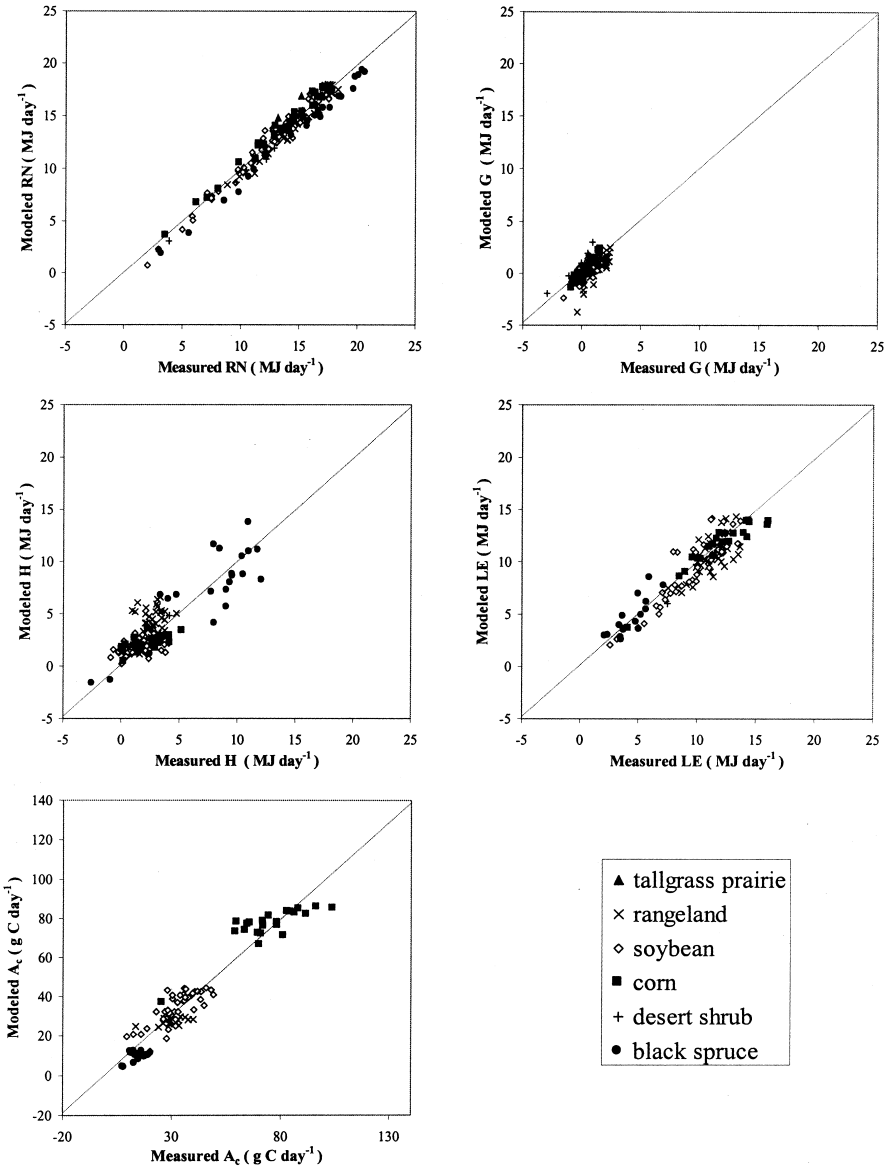

Fig. 7. Comparison of daily-integrated measurements of system latent heating and canopy carbon assimilation made in six different vegetative stands with estimates generated by the ALEX model.

values for *G* tend to accumulate in *H*, leaving *LE* unaffected.

Because we have used LUE values based on seasonal dry matter accumulation, we expect Eq. (11) to underestimate daytime hourly carbon fluxes to some degree (see Section 3.3). This effect is particularly evident for black spruce (Fig. 6), which has a high respiration to assimilation ratio. The bias is reduced somewhat on the daily timescale. A comparison with daily (24 h) integrated energy and carbon fluxes from all measurement datasets is shown in Fig. 7, with related statistics in Table 4. The MAPD values for daily-integrated flux estimates from the ALEX model, averaged over all datasets, are 6% (*RN*), 12% (*LE*), and

Table 4
Quantitative measures of model performance in estimating daily-integrated carbon and heat fluxes[a]

Flux	N	O	S_o	RMSD	MBE	a	b	R^2	MAPD
A_c	102	37.9	22.4	6.7	−0.1	0.0	1.00	0.92	18
RN	166	13.3	3.8	0.8	−0.3	−0.4	1.01	0.96	6
LE	128	9.9	3.1	1.3	−0.4	0.4	0.92	0.85	12
H	135	2.9	2.8	1.6	0.6	1.1	0.81	0.71	197
G	142	0.7	0.9	0.8	−0.1	0.0	0.80	0.46	161

[a] N, O, S_o, RMSD, MBE, a, b and R^2 are defined as in Table 1. MAPD is the mean-absolute-percent-difference between observed and modeled daily-integrated fluxes. The terms N, b, R^2 and MAPD are unitless; O, S_o, RMSD, MBE, and a have units of g C per day for A_c and units of MJ per day for *RN*, *LE*, *H* and *G*.

18% (A_c). We note that net carbon fluxes over black spruce are still underestimated, even in a daily average. For reasonable daily estimates of carbon uptake, the net LUE for spruce must be adjusted to compensate for seasonal variations in the respiration to assimilation ratio.

5. Conclusions

A simple analytical model for predicting carbon assimilation fluxes and canopy transpiration based on stand-level measurements of canopy LUE has been developed and tested in comparison with measurements made over canopies of a variety of C_3 and C_4 plant species. Comparisons between modeled and measured evapotranspiration (*LE*) and carbon assimilation (A_c) fluxes yield mean-absolute-percent-differences of 24% (*LE*) and 33% (A_c) for hourly daytime fluxes, and 12% (*LE*) and 18% (A_c) for daily-integrated fluxes. The analytical model also reasonably captures observed phenomena such as moisture stress effects on stomatal conductance and modulation of canopy LUE due to diurnal variations in insolation composition and VPD.

With these measurement datasets, we found that the simple semi-empirical model described here performed as well and often better than the more detailed, process-based Cupid model. This finding illustrates an interesting point made by Jarvis (1993), who notes that 'bottom-up models', constructed from detailed mechanistic representations of leaf-level processes and scaled to the canopy level, are often more susceptible to errors in inputs and scaling assumptions than are 'top-down' models, which are constrained 'to the realm of observation' by some relationship developed at the stand level. In the simple model, assimilation (and therefore canopy resistance) is semi-constrained (but not rigidly fixed) by a quantity that has been found to be conservative in nature: the canopy LUE. Even if small errors occur on an hourly timestep, the daily or seasonal integral of carbon uptake will generally be properly constrained under this approach, and these are in many applications the flux timescales of interest.

Jarvis (1993) warns, however, that top-down models such as this have usefulness only within the range of conditions under which the embedded empiricisms were developed. We have no assurance, for example, that this model as it is given here will perform well in predicting regional fluxes under conditions of elevated CO_2. For such studies, a synthesis between top-down and bottom-up modeling may be optimal. A process-based model such as Cupid can be used to modify slowly-evolving empirical relationships (such as the β versus C_i relationship in Eq. (10)) embedded in the analytical model, which can then be employed more efficiently at finer spatial and temporal resolution.

Acknowledgements

This research was supported by NASA Grants NAGW-4138 and NAG5-2877, with the assistance of the University of Wisconsin Agricultural Experiment Station. The authors are indebted to many individuals who participated in the planning and implementation of the FIFE experiment; among them: F.G. Hall (NASA), P.J. Sellers (NASA), and R.E. Murphy (NASA); the FIFE Information System team, led by D.E. Strebel of Versar Inc.; and the researchers responsible for the micrometeorological and surface flux measurements used in this analysis: S.B. Verma and J. Kim. The authors also acknowledge the planners and participants in the SGP '97 field campaign, including T.J. Jackson (USDA ARS) and M.Y. Wei (NASA). Special thanks are extended to T.P. Meyers for providing flux and meteorological measurements taken at the Little Washita and Champaign IL sites, and W.P. Kustas for providing measurements from MONSOON '90.

Appendix A. The ALEX model

ALEX, in its most basic form, is a two-source (soil and vegetation) model of heat, water and carbon exchange between a vegetated surface and the atmosphere. The net energy balance at the earth's surface can be represented by

$$RN = H + LE + G \tag{A.1}$$

where RN is the net radiation above the surface, and H, LE, and G are the fluxes of sensible, latent, and soil conduction heating, respectively. The set of equations defining energy fluxes ($W\,m^{-2}$) in the ALEX model (see Fig. 1) is as follows:

Net Radiation:

$$RN = RN_c + RN_s \tag{A.2}$$

$$RN_c = H_c + LE_c \tag{A.3}$$

$$RN_s = H_s + LE_s + G \tag{A.4}$$

Sensible Heat:

$$H = H_c + H_s \tag{A.5}$$

$$H = \rho c_p \frac{T_{ac} - T_a}{R_a} \tag{A.6}$$

$$H_s = \rho c_p \frac{T_s - T_{ac}}{R_s} \tag{A.7}$$

$$H_c = \rho c_p \frac{T_c - T_{ac}}{R_x} \tag{A.8}$$

Latent Heat:

$$LE = LE_c + LE_s \tag{A.9}$$

$$LE = \frac{\rho c_p\, e_{ac} - e_a}{\gamma_p \quad R_a} \tag{A.10}$$

$$LE_s = \frac{\rho c_p\, e_s - e_{ac}}{\gamma_p \quad R_s} \tag{A.11}$$

$$LE_c = LE_{ce} + LE_{ct} \tag{A.12}$$

$$LE_{ce} = \frac{\rho c_p\, e*(T_c) - e_a}{\gamma_p \quad R_x / f_{wet}} \tag{A.13}$$

$$LE_{ct} = f\,[T_c, e_{ac}] \quad \text{(Light-use efficiency submodel)} \tag{A.14}$$

Soil Heat:

$$G = f\,[T(z), \theta(z)] \quad \text{(Soil transport submodel)} \tag{A.15}$$

where T is temperature (K), e is vapor pressure (kPa), R is the transport resistance ($s\,m^{-1}$), ρ is the density of air ($kg\,m^{-3}$), c_p is the heat capacity of air at constant pressure ($J\,kg^{-1}\,K^{-1}$) and γ_p is the psychometric constant ($kPa\,K^{-1}$).

The subscripts 'a', 'ac', and 'x' signify properties of the air above and within the canopy, and within the leaf boundary layer, respectively, while 's' and 'c' refer to fluxes and states associated with the soil and canopy components of the system. The resistance terms (R) are defined in the main text (Section 3.1; note that in Section 3, resistance is expressed in units of $m^2\,s\,\mu mol^{-1}$).

The soil and canopy energy budgets are fueled by the net radiation apportioned to each component (RN_s and RN_c, respectively). In ALEX, we have adopted a simple, analytical method for partitioning net radiation that depends on leaf and soil optical properties and on the canopy leaf area index; this strategy is outlined in Appendix B.

Canopy transpiration (LE_{ct}) and soil heat conduction (G) flux estimates are generated by submodels within ALEX, as indicated by the functional expressions in Eqs. (A.14) and (A.15). The transpiration submodel is described in Section 3.1 in the main text. The flux of heat conducted into the soil surface is computed by a multi-layer numerical soil model that serves as the lower boundary to ALEX, described briefly further (Section A.l). This model also provides an estimate of the vapor pressure at the soil surface (e_s), used in predicting the soil evaporation rate (Eq. (A.11)). The canopy evaporation flux (LE_{ce}) arises from the fraction of total leaf area (F) that is covered by liquid water (f_{wet}), as discussed in Section A.2.

A.1. Soil transport submodel

The treatment of heat and water transport through the soil profile in ALEX is a generalization of algorithms from Campbell (1985), adapted to a soil structure with layered hydraulic and thermal properties. Profiles of soil temperature, $T(z)$, and water content, $\theta(z)$, with depth z are updated by solving systems of second-order, time-dependent differential

equations using a Newton–Raphson finite-difference solution technique. The temperature and water content at the soil surface form the interface condition between transport in the soil and exchanges in the vegetative canopy.

A.1.1. Heat

The soil temperature profile (including the surface temperature T_s) and the conduction flux of heat through the soil profile (including the surface heat flux, G) are obtained as the solution to the time-dependent differential equation for heat flow:

$$\rho_s c_s \frac{\partial T}{\partial t} = \frac{\partial}{\partial z}\left(\lambda_s \frac{\partial T}{\partial z}\right) + Q_H \tag{A.16}$$

where t is the time (s), z is the depth below the surface (m); $\rho_s c_s$ is the volumetric soil heat capacity ($J\,m^{-3}\,K^{-1}$), λ_s is the soil thermal conductivity ($J\,m^{-1}\,s^{-1}\,K^{-1}$), Q_H is the heat source term given by $(RN_s - LE_s)/\Delta z$ ($W\,m^{-3}$) at the soil surface and Δz is the thickness of the surface soil layer (m). The soil surface heat flux is obtained by integrating Eq. (A.16) over the surface layer:

$$G = \rho_s c_s \,\Delta z \frac{\partial T}{\partial t}\bigg|_{z=0} + \lambda_s \frac{\partial T}{\partial z}\bigg|_{z=0}. \tag{A.17}$$

Because thermal conductivity is a non-linear function of soil water content, the system of layer temperature equations (A.16) must be solved in iteration with the soil water profile.

A.1.2. Water

The time rate of change in soil water content with depth is given by Richard's Equation:

$$\frac{\partial \theta}{\partial t} = \frac{\partial}{\partial z}\left(K_w \frac{\partial \psi}{\partial z} - K_w g\right) - U \tag{A.18}$$

where θ is the volumetric water content ($m^3\,m^{-3}$), K_w is the soil hydraulic conductivity ($kg\,s\,m^{-3}$); ψ is the soil water potential ($J\,kg^{-1}$), g is the gravity ($m\,s^{-2}$), $K_w g$ is the drainage due to gravitational forces ($kg\,m^{-2}\,s^{-1}$) and U is the volumetric water sink ($kg\,m^{-3}\,s^{-1}$). At the soil surface, U accounts for the difference between soil evaporation and infiltration rates. Below the surface, it represents the water extracted from a given soil layer by plant roots.

Plants will extract the most water from those soil layers that contain the greatest density of roots (Campbell, 1985). Roots tend to have an exponential distribution with depth in the soil, so the fraction of active roots between depth z and depth $z+\Delta z$ can be approximated with

$$F_{root}(z) = \frac{e^{-\tau z} - e^{-\tau(z+\Delta z)}}{1 - e^{-\tau d_r}} \tag{A.19}$$

where d_r is the depth of rooting (m) and τ is the empirical distribution coefficient (Norman and Campbell, 1983).

This distribution scheme places most of the roots in the upper layers of the soil, as has been observed in many studies. As written, $F_{root}(z)$ is normalized to sum to unity over the rooting depth (d_r). If any layer of thickness Δz is depleted of available water, then d_r in Eq. (A.19) is replaced by $d_r - \Delta z$, and $F_{root}(z)$ for that layer becomes zero. The root uptake function used in ALEX is

$$U(z) = \frac{LE_{ct}' \times F_{root}(z)}{\lambda_k \Delta z} \tag{A.20}$$

where λ_k is the latent heat of vaporization ($J\,kg^{-1}$) and LE_{ct}' is the transpiration rate reduced by soil water limitations ($W\,m^{-2}$; Eq. (17) in the main text).

Under heavy rainfall, the cumulative precipitation transmitted to the soil surface during a given timestep may exceed the surface infiltration capacity. In such cases, the excess water can either be temporarily ponded and saved for infiltration during subsequent tiinesteps, or it can be extracted from the modeling site in the form of runoff. The fate of excess water is likely to be determined by the local topography of the site: whether it is on a slope or in a basin. In ALEX, we define a soil surface storage capacity: the maximum depth of water, h_{max} (mm), that can be stored on the surface before runoff occurs. If the site is in a basin where ponding is allowed, surface storage is effectively unlimited. If not, the soil water potential at the soil surface is constrained to be less than or equal to some small positive value corresponding to the head h_{max}. The surface source term in Eq. (A.18) is adjusted until this is the case; all excess standing water is routed into runoff.

A.2. Canopy evaporation/dew deposition

During light precipitation events over a dense canopy, there can be significant potential for interception and re-evaporation of rain or irrigation waters over relatively short time scales. Following Sellers et al. (1996), the maximum canopy interception store (W_{imax}; mm) is presumed to be a linear function of the leaf area index (F):

$$W_{\mathrm{i\,max}} = 2 \times W_{\mathrm{i\,max}} \times F, \tag{A.21}$$

where W_{imax} is the maximum potential reservoir (in mm) per unit single-sided leaf area, and we assume that both sides of each leaf will be wetted equally. Incident precipitation (W_{o}) is partitioned between canopy interception and soil application based on the vegetation cover fraction (f_{c}) until this interception reservoir is filled:

$$W_{\mathrm{i}} = \min(f_{\mathrm{c}} \times W_{\mathrm{o}}, W_{\mathrm{i\,max}}); \tag{A.22}$$

any additional precipitation is transmitted to the soil surface and attributed to U (Eq. (A.18)). For precipitation falling vertically, the relevant cover fraction is an exponential function of leaf area index:

$$f_{\mathrm{c}} = 1 - \exp(-0.5F) \tag{A.23}$$

where we have assumed a random, spherical leaf angle distribution.

Intercepted water typically will not coat the leaf uniformly; beads tend to form, leaving parts of the leaf free from standing water and stomata unblocked to transpiration and assimilation fluxes. In ALEX, the fraction of leaf area covered with water (f_{wet}) grows linearly with intercepted precipitation to some maximum allowed value ($f_{\mathrm{wet\,max}}$) attained when the interception reservoir is filled (W_{i}=$W_{\mathrm{i\,max}}$) the remainder of the canopy is presumed to be dry:

$$f_{\mathrm{wet}} = \frac{W_{\mathrm{i}}}{W_{\mathrm{i\,max}}} f_{\mathrm{wet\,max}}, \tag{A.24}$$

$$f_{\mathrm{dry}} = 1 - f_{\mathrm{wet}}. \tag{A.25}$$

The boundary layer resistance to evaporation from this leaf-surface water pool must take this wetted leaf area fraction into account:

$$LE_{\mathrm{ce}} = \frac{\rho c_{\mathrm{p}} [e*(T_{\mathrm{c}}) - e_{\mathrm{ac}}]}{\lambda \quad R_{\mathrm{x}}/f_{\mathrm{wet}}}. \tag{A.26}$$

When conditions in the canopy are conducive to dew deposition ($e^*(T_{\mathrm{c}}) < e_{\mathrm{ac}}$), the total leaf area participates and the factor f_{wet} is omitted from Eq. (A.26).

Appendix B. Approximations for net radiation and absorbed PAR

Net radiation and absorbed PAR are modeled in ALEX using an analytical formalism describing light interception by canopies developed by Goudriaan (1977) and outlined by Monteith and Unsworth (1990) and by Campbell and Norman (1998). Assuming that the leaf reflectance and transmittance factors are equal, simple approximations for canopy reflectance and transmittance can be constructed involving only leaf absorptivity, soil reflectance, canopy leaf area index (LAI) and leaf angle distribution (LAD). Goudriaan (1977) showed that these approximations work well over a range of leaf and canopy properties, and for solar zenith angles less than the mean leaf inclination angle (60° in the case of a spherical LAD). They include the effects of reflection at the soil surface and re-reflection by leaves, which can be important in sparse canopies, serving to enhance the downwelling radiation field.

Given measurements or estimates of LAI, LAD, leaf absorptivity in the visible, near infrared (NIR) and thermal wavebands, and soil reflectance in the visible and NIR, canopy transmittance factors τ_{bv}, τ_{dv}, τ_{bn}, τ_{dn}, and τ_{dl}, and reflectance factors ρ_{bv}, ρ_{bn}, ρ_{dn}, and ρ_{dl} can be computed using these approximations. Here, subscripts ‘v’, ‘n’, and ‘l’ signify the visible, NIR and thermal wavebands, and subscripts ‘b’ and ‘d’ indicate response to direct beam and diffuse radiation components, respectively. Vegetation clumping in canopies can be accommodated by modifying the LAI used in the calculation of extinction coefficients by a ‘clumping factor’ (Chen and Cihlar, 1995; Campbell and Norman, 1998).

Weiss and Norman (1985) summarize a methodology for partitioning measurements of solar irradiance (S) into visible and NIR waveband components (S_{v} and S_{n}), and further into diffuse and direct beam components (S_{dv}, S_{dn}, S_{bv}, and S_{bn}). Using the resulting partitioning factors, defined here as

$$f_v = \frac{S_v}{S} \quad f_{dv} = \frac{S_{dv}}{S_v} \quad f_{dn} = \frac{S_{dn}}{S_n} \quad f_n = \frac{S_n}{S}$$
$$f_{bv} = \frac{S_{bv}}{S_v} \quad f_{bn} = \frac{S_{bn}}{S_n}, \tag{B.1}$$

a radiation-weighted surface albedo can be obtained:

$$\alpha_{sfc} = f_v(f_{dv} \times \rho_{dv} + f_{bv} \times \rho_{bv}) + f_n(f_{dn} \times \rho_{dn} + f_{bn} \times \rho_{bn}) \tag{B.2}$$

Given these canopy reflectance and transmittance coefficients and estimates of the soil reflectivity in the visible, NIR and thermal wavebands (ρ_{sv}, ρ_{sn}, and ρ_{sl}, respectively), the net radiation above the canopy (RN) and above the soil surface (RN_s), and the divergence of net radiation within the canopy (RN_c) can be approximated with

$$RN = (L_\downarrow - L_\uparrow) + (S_\downarrow - S_\uparrow) \approx L_{sky}(1 - \rho_{dl} - \tau_{dl}^2\rho_{sl}) - L_c(1 + \tau_{dl}\rho_{sl}) - L_s\tau_{dl} + (1 - \alpha_{sfc})S \tag{B.3}$$

$$RN_s = (L_{\downarrow s} - L_{\uparrow s}) + (S_{\downarrow s} - S_{\uparrow s}) \approx L_{sky}\tau_{dl}(1 - \rho_{sl}) + L_c(1 - \rho_{sl}) - L_s(1 - \rho_{dl}) + [\tau_{bv}S_{bv} + \tau_{dv}S_{dv}](1 - \rho_{sv}) + [\tau_{bn}S_{bn} + \tau_{dn}S_{dn}](1 - \rho_{sn}) \tag{B.4}$$

$$RN_c = RN - RN_s. \tag{B.5}$$

The longwave components of RN and RN_s are functions of the thermal radiation emitted by the sky ($L_{sky} = \varepsilon_{sky}\sigma T_a^4$, where σ is the Stefan-Boltzmann coefficient and ε_{sky} is the sky emissivity), the canopy ($L_c = \varepsilon_c\sigma T_c^4$; ε_c is the canopy emissivity) and the soil ($L_s = \varepsilon_s\sigma T_s^4$; ε_s is the soil emissivity). Here we have retained only those components that are first or lower order in thermal reflectivity; however, because the coefficient of diffuse thermal radiation transmission through the canopy will approach unity for sparse vegetation, the second order component in τ_{dl} is also retained. Following Monteith and Unsworth (1990), atmospheric emissivity is approximated as a weighted average of clear and cloudy values, weighted by the fraction of sky cloud cover. We use the empirical formula of Brutsaert (1984) for estimating clear sky emissivity, and assume a cloud emissivity of 1. The soil emissivity is given by $\varepsilon_s = 1 - \rho_{sl}$, and the canopy emissivity by $\varepsilon_c = 1 - \rho_{dl} - \tau_{dl}$. The shortwave components of net radiation depend on insolation values above the canopy (S) and above the soil surface, the reflectivity of the soil-canopy system (α_{sfc}) and the soil surface in the visible and NIR bands ($\rho_{s,v}$ and $\rho_{s,n}$).

The PAR radiation absorbed by green leaves in the vegetation canopy can be approximated with

$$\begin{aligned} \mathrm{PAR} &= f_v SA \\ \mathrm{PAR_b} &= \left[1 - \rho_{bv} - \tau_{bv}\left(1 - \rho_{s,v}\right)\right] f_{bv}\mathrm{PAR} \\ \mathrm{APAR_d} &= \left[1 - \rho_{dv} - \tau_{dv}\left(1 - \rho_{s,v}\right)\right] f_{dv}\mathrm{PAR} \\ \mathrm{APAR} &= f_g \times (\mathrm{APAR_b} + \mathrm{APAR_d}). \end{aligned} \tag{B.6}$$

References

Anderson, M.C., Norman, J.M., Diak, G.R., Kustas, W.P., Mecikalski, J.R., 1997. A two-source time-integrated model for estimating surface fluxes using thermal infrared remote sensing. Remote Sensing Environ. 60, 195–216.

Aphalo, P.J., Jarvis, P.G., 1991. Do stomata respond to relative humidity? Plant, Cell Environ. 14, 127–132.

Avissar, R., Pielke, R.A., 1991. The impact of plant stomatal control on mesoscale atmospheric circulations. Agric. For. Meteorol. 54, 353–372.

Baldocchi, D., 1994. An analytical solution for coupled leaf photosynthesis and stomatal conductance models. Tree Physiol. 14, 1069–1079.

Baldocchi, D.D., Meyers, T.P., 1998. On using ecophysiological, micrometeorological and biogeochemical theory to evaluate carbon dioxide, water vapor and trace gas fluxes over vegetation: a perspective. Agric. For. Meteorol. 90, 1–26.

Ball, J.T., 1988. An analysis of stomatal conductance. Ph.D. Thesis, Stanford University.

Ball, J.T., Woodrow, I.E., Berry, J.A., 1987. A model predicting stomatal conductance and its contribution to the control of photosynthesis under different environmental conditions. In: Biggins, J. (Ed.), Progress in Photosynthesis Research. Nijhoff, Dodrecht, pp. 221–225.

Brutsaert, W., 1984. Evaporation into the Atmosphere: Theory, History and Applications. D. Reidel, Boston.

Campbell, G.S., 1985. Soil physics with BASIC — Transport Models for Soil–Plant Systems. Elsevier, New York.

Campbell, G.S., Norman, J.M., 1998. An Introduction to Environmental Biophysics. Springer, New York.

Chen, J.M., Cihlar, J., 1995. Quantifying the effect of canopy architecture on optical measurements of leaf area index using two gap size methods. IEEE Trans. Geosci. Remote Sensing 33, 777–787.

Collatz, G.J., Ball, J.T., Grivet, C., Berry, J.A., 1991. Physiological and environmental regulation of stomatal conductance, photosynthesis and transpiration: a model that includes a laminar boundary layer. Agric. For. Meteorol. 54, 107–136.

Collatz, G.J., Ribas-Carbo, J., Berry, J.A., 1992. Coupled photosynthesis-stomatal conductance model for leaves of C_4 plants. Aust. J. Plant Physiol. 19, 519–538.

Daughtry, C.S.T., Gallow, K.P., Bauer, M.E., 1983. Spectral estimates of solar radiation intercepted by corn canopies. Agron. J. 75, 527–531.

Dickinson, R.E., Henderson-Sellers, A., Rosenzweig, C., Sellers, P.J., 1991. Evapotranspiration models with canopy resistance for use in climate models, a review. Agric. For. Meteorol. 54, 373–388.

Duncan, W.G., 1971. Leaf angles, leaf area and canopy photosynthesis. Crop Sci. 11, 482–485.

Field, C.B., 1991. Ecological scaling of carbon gain to stress and resource availability. In: Mooney, H.A., Winner, W.E., Pell, E.J. (Eds.), Response of Plants to Multiple Stresses. Academic Press, San Diego, pp. 35–65.

Friend, A.D., 1991. Use of a model of photosynthesis and leaf microenvironment to predict optimal stomatal conductance and leaf nitrogen partitioning. Plant, Cell Environ. 14, 895–905.

Fritschen, L.J. et al., 1992. Comparisons of surface flux measurement systems used in FIFE 1989. J. Geophys. Res. 97, 18,697–18,713.

Goetz, S.J., Prince, S.D., 1998a. Modeling terrestrial carbon exchange and storage: the evidence for and implications of functional convergence in light use efficiency. In: Fitter, A.H., Raffaelli, D. (Eds.), Advances in Ecological Research. Academic Press, San Diego, pp. 57–92.

Goetz, S.J., Prince, S.D., 1998b. Variability in carbon exchange and light utilization among boreal forest stands: implications for remote sensing of net primary production. Can. J. For. Res. 28, 375–389.

Gollan, T., Passioura, J.B., Munns, R., 1986. Soil water status affects the stomatal conductance of fully turgid wheat and sunflower leaves. Aust. J. Plant Physiol. 13, 459–464.

Goudriaan, J., 1977. Crop micrometeorology: a simulation study. Simulation Monographs, Wageningen.

Goulden, M.L., Crill, P.M., 1997. Automated measurements of CO_2 exchange at the moss surface of a black spruce forest. Tree Physiol. 17, 537–542.

Goulden, M.L. et al., 1997. Physiological responses of a black spruce forest to weather. J. Geophys. Res. D24, 28,987–28,996.

Gower, S.T., Kucharik, C.J., Norman, J.M., 1999. Direct and indirect estimation of leaf area index, f_{APAR} and net primary production of terrestrial ecosystems. Remote Sensing Environ. 70, 29–51.

Griffin, K.L., 1994. Calorimetric estimates of construction cost and their use in ecological studies. Func. Ecol. 8, 551–562.

Gutschick, V.P., 1996. Physiological control of evapotranspiration by shrubs: scaling measurements from leaf to stand with the aid of comprehensive models. In. Barrow, J.R., McArthur, E.D., Sosebee, R.E., Tausch, R.J. (Eds.), Proc. Shrubland Ecosystem Dynamics in a Changing Environment, Las Cruces, NM.

Haxeltine, A., Prentice, I.C., 1996. A general model for the light-use efficiency of primary production. Func. Ecol. 10, 551–561.

Hesketh, J., Baker, D., 1969. Light and carbon assimilation by plant communities. Crop Sci. 7, 285–293.

Jackson, T., 1997. Experiment Plan: Southern Great Plains 1997 (5GP97) Hydrology Experiment, USDA-ARS Hydrology Laboratory, Beltsville, MD.

Jarvis, P.G., 1976. The interpretation of the variations in leaf water potential and stomatal conductance found in canopies in the field. Philos. Trans. R. Soc. London Ser. B 273, 593–610.

Jarvis, P.G., 1993. Prospects for bottom-up models. In: Ehleringer, J.R., Field, C.B. (Eds.), Sealing Physiological Processes Leaf to Globe. Academic Press, San Diego, pp. 115–126.

Kim, J., Verma, S.B., 1990a. Carbon dioxide exchange in a temperate grassland ecosystem. Boundary-Layer Meteorol. 52, 135–149.

Kim, J., Verma, S.B., 1990b. Components of surface energy balance in a temperate grassland ecosystem. Boundary-Layer Meteorol. 51, 401–417.

Kumar, M., Monteith, J.L., 1981. Remote sensing of plant growth. In: Huxley, P.A. (Ed.), Plants and the Daylight Spectrum. International Council for Research in Agroforestry, Nairobi, pp. 347–364.

Kustas, W.P., Goodrich, D.C., 1994. Preface, MONSOON '90 Multidisciplinary Experiment. Water Resources Res. 30, 1211–1225.

Kustas, W.P., Norman, J.M., 1997. A two-source approach for estimating turbulent fluxes using multiple angle thermal infrared observations. Water Resources Res. 33, 1495–1508.

Kustas, W.P., Norman, J.M., Schmugge, T.J., Anderson, M.C., 2000. Mapping surface energy fluxes with radiometric temperature. In: Quattrochi, D.A., Luvall, J.C. (Eds.), Remote Sensing in Land Surface Processes, in press.

Landsberg, J.J., Hingston, F.J., 1996. Evaluating a simple radiation/dry matter conversion model using data from Eucalyptus globulus plantations in Western Australia. Tree Physiol. 16, 801–808.

Landsberg, J.J. et al., 1997. Energy conversion and use in forests: the analysis of forest production in terms of radiation utilisation efficiency (ε). In: Gholtz, H.L., Nakane, K., Shimoda, H. (Eds.), Use of Remote Sensing in the Modeling of Forest Productivity. Kluwer Academic Publishers, New York, pp. 273–298.

Lawford, R.G., 1999. A midterm report on the GEWEX Continental-Scale International Project (GCIP). J. Geophys. Res. 104 (D16), 19,279–19,292.

Leuning, R., 1990. Modeling stomatal behavior and photosynthesis of *Eucalyptus grandis*. Aust. J. Plant Physiol. 17, 159–175.

Leuning, R., 1995. A critical appraisal of a combined stomatal-photosynthesis model for C_3 plants. Plant, Cell Environ. 18, 339–355.

Leverenz, J.W., Jarvis, P.G., 1979. Photosynthesis in Sitka spruce VIII. The effects of light flux density and direction on the rate of net photosynthesis and the stomatal conductance of needles. J. Appl. Ecol. 16, 919–932.

Lloyd, J., 1991. Modeling stomatal responses to environment in *Macadamia integrifolia*. Aust. J. Plant Pathol. 18, 649–660.

Long, S.P., Hutchin, P.R., 1991. Primary productivity in grasslands and coniferous forests with climate change: an overview. Ecol. Applications 12, 139–156.

Mascart, P., Taconet, O., Pinty, J., Mehrez, M.B., 1991. Canopy resistance formulation and its effect in mesoscale models: a HAPEX perspective. Agric. For. Meteorol. 54, 319–351.

McNaughton, K.G., Jarvis, P.G., 1991. Effects of spatial scale on stomatal control of transpiration. Agric. For. Meteorol. 54, 269–301.

Moncrieff, J.B., Verma, S.B., Cook, D.R., 1992. Intercomparison of eddy correlation carbon dioxide sensors during FIFE 1989. J. Geophys. Res. 97, 18,725–18,730.

Monteith, J.L., 1966. The photosynthesis and transpiration of crops. Exp. Agric. 2, 1–14.

Monteith, J.L., 1972. Solar radiation and production in tropical ecosystems. J. Appl. Ecol. 9, 747–766.

Monteith, J.L., 1995. A reinterpretation of stomatal responses to humidity. Plant, Cell Environ. 18, 357–364.

Monteith, J.L., Unsworth, M.H., 1990. Principles of Environmental Physics. Edward Arnold Publishers, London, 291 pp.

Mott, K.A., Parkhurst, D.F., 1991. Stomatal response to humidity in air and helox. Plant, Cell Environ. 14, 509–515.

Myneni, R.B., Hall, F.G., Sellers, P.J., Marshak, A.L., 1995a. The interpretation of spectral vegetation indices. IEEE Trans. Geosci. Remote Sensing 33, 481–486.

Myneni, R.B., Maggion, S., Iaquinta, J. et al., 1995b. Optical remote sensing of vegetation: modeling, caveats, and algorithms. Remote Sensing Environ. 51, 169–188.

Nie, D. et al., 1992. An intercomparison of surface energy flux measurement systems used during FIFE 1987. J. Geophys. Res. 97, 18,715–18,724.

Norman, J.M., 1979. Modeling the complete crop canopy. In: Barfield, B.J., Gerber, J.F. (Eds.), Modification of the Aerial Environment of Plants. Am. Soc. Agric. Eng., St. Joseph, pp. 249–277.

Norman, J.M., 1993. Scaling processes between leaf and canopy levels. Scaling Physiological Processes: Leaf to Globe. Academic Press, New York, pp. 41–76.

Norman, J.M., Arkebauer, T.J., 1991. Predicting canopy light-use efficiency from leaf characteristics. Modeling Plant and Soil Systems, Agronomy Monograph No. 31. ASA-CSSA-SSSA, Madison, pp. 125–143.

Norman, J.M., Campbell, G., 1983. Application of a plant-environment model to problems in irrigation. In: Hillel, D. (Ed.), Advances in Irrigation. Academic Press, New York, pp. 156–188.

Norman, J.M., Garcia, R., Verma, S.B., 1992. Soil surface CO_2 fluxes and the carbon budget of a grassland. J. Geophys. Res. 97, 18,845–18,853.

Norman, J.M., Kustas, W.P., Humes, K.S., 1995. A two-source approach for estimating soil and vegetation energy fluxes from observations of directional radiometric surface temperature. Agric. For. Meteorol. 77, 263–293.

Norman, J.M., Polley, W.R., 1989. Canopy photosynthesis. In: Briggs, W.R. (Ed.), Photosynthesis. Alan R. Liss, Inc., New York, pp. 227–241.

Potter, C.S. et al., 1993. Terrestrial ecosystem production: a process model based on global satellite and surface data. Global Biogeochem. Cycles 7, 811–841.

Press, W.H., Teukolsky, S.A., Vetterling, W.T., Flannery, B.P., 1992. Numerical Recipes in C. Cambridge University Press, Cambridge.

Prince, S.D., Goward, S.J., 1995. Global primary production: a remote sensing approach. J. Biogeo. 22, 815–835.

Puckridge, D.W., Donald, C.M., 1967. Competition among wheat plants sown at a wide range of densities. Aust. J. Agric. Res. 18, 193–211.

Randall, D.A. et al., 1996. A revised land surface parameterization (SiB2) for GCMs Part III. The greening of the Colorado State University General Circulation Model. J. Climate 9, 738–763.

Ruimy, A., Dedieu, G., Saugier, B., 1994. Methodology for the estimation of terrestrial net primary production from remotely sensed data. J. Geophys. Res. 99, 5263–5283.

Runyon, J., Waring, R.H., Goward, S.N., Welles, J.M., 1994. Environmental limits on net primary production and light-use efficiency across the Oregon transect. Ecol. Applications 4, 226–237.

Ryan, M.G., Lavigne, M.B., Gower, S.T., 1997. Annual carbon cost of autotrophic respiration in boreal forest ecosystems in relation to species and climate. J. Geophys. Res. 28,871–28, 883.

Sellers, P.J., Hall, F.G., Asrar, G., Strebel, D.E., Murphy, R.E., 1992. An overview of the first international satellite land surface climatology project (ISLSCP) field experiment (FIFE). J. Geophys. Res. 97, 18,345–18,371.

Sellers, P.J. et al., 1995. The Boreal Ecosystem-Atmosphere Study (BOREAS): an overview and early results from the 1994 field year. Bull. Am. Meteorol. Soc. 76: 1549–1577.

Sellers, P.J. et al., 1996. A revised land surface parameterization (SiB2) for atmospheric GCMs Part I. Model formulation. J. Climate 9, 676–705.

Stannard, D.I., 1988. Use of a hemispherical chamber for measurement of evapotranspiration. U.S. Geological Survey Open File Report 88–452, l8 pp.

Steinmetz, S., Guerif, M., DeLecolle, R., F, B., 1990. Spectral estimates of the photosynthetically active radiation and light-use efficiency of a winter-wheat crop subjected to nitrogen and water deficiences. Int. J. Remote Sensing 11, 1797–1808.

Strebel, D.E., Landis, D.R., Huemmrich, K.F., Meeson, B.W., 1994. Collected data of the first ISLSCP field experiment Vol. 1. Surface observations and non-image data sets, published on CD-ROM by NASA.

Sutton, D.J., Goulden, M.L., Wofsy, S.C., 1998. BOREAS TF-03 NSA-OBS Tower Flux, Meteorological, and Soil Temperature Data.Available online at [http://www-eosdis.ornl.gov/] from the ORNL Distributed Active Archive Center, Oak Ridge National Laboratory, Oak Ridge, Tennessee, USA.

Twine, T.E., 1998. Underestimation of eddy covariance fluxes over a grassland. M.S. Thesis, University of Wisconsin-Madison, Madison, 58 pp.

Vertregt, N., Penning de Vries, F.W.T., 1987. A rapid method for determining the efficiency of biosynthesis of plant biomass. J. Theor. Biol. 128, 109–119.

Wagai, R., Brye, K.R., Gower, S.T., Norman, J.M., Bundy, L.G., 1998. Land use and environmental factors influencing soil surface CO_2 flux and microbial biomass in natural and managed ecosystems in southern Wisconsin. Soil Biol. Biochem. 30, 1501–1509.

Weiss, A., Norman, J.M., 1985. Partitioning solar radiation into direct and diffuse, visible and near-infrared components. Agric. For. Meteorol. 34, 205–213.

Wong, S.C., Cowan, I.R., Farquhar, G.D., 1979. Stomatal conductance correlates with photosynthetic capacity. Nature 282, 424–426.